



Since January 2020 Elsevier has created a COVID-19 resource centre with free information in English and Mandarin on the novel coronavirus COVID-19. The COVID-19 resource centre is hosted on Elsevier Connect, the company's public news and information website.

Elsevier hereby grants permission to make all its COVID-19-related research that is available on the COVID-19 resource centre - including this research content - immediately available in PubMed Central and other publicly funded repositories, such as the WHO COVID database with rights for unrestricted research re-use and analyses in any form or by any means with acknowledgement of the original source. These permissions are granted for free by Elsevier for as long as the COVID-19 resource centre remains active.

## Chapter 23

# Lung, Pleura, and Mediastinum

Ronald A. Herbert<sup>1</sup>, Kyathanahalli S. Janardhan<sup>2</sup>, Arun R. Pandiri<sup>1</sup>, Mark F. Cesta<sup>1</sup>, Vivian Chen<sup>3</sup> and Rodney A. Miller<sup>4</sup>

<sup>1</sup>National Institute of Environmental Health Sciences, Research Triangle Park, NC, United States, <sup>2</sup>Integrated Laboratory Systems Inc., Research Triangle Park, NC, United States, <sup>3</sup>Charles River Laboratories – Pathology Associates, Durham, NC, United States, <sup>4</sup>Experimental Pathology Laboratories, Inc., Research Triangle Park, NC, United States

### Chapter Outline

<b>1 Introduction</b>	<b>437</b>	5.5 Mineral	448
<b>2 Normal Lung</b>	<b>438</b>	5.6 Pigments	448
2.1 Embryology	438	5.7 Inflammatory Lesions	448
2.2 Anatomy	439	<b>6 Nonneoplastic and Neoplastic Proliferative Lesions</b>	<b>448</b>
2.3 Histology	440	6.1 Regenerative Hyperplasia	449
2.3.1 Trachea, Bronchi, and Bronchioles	440	6.2 Primary Hyperplasia of the Alveolar Epithelium	450
2.3.2 Terminal Bronchioles	441	6.3 Bronchial Hyperplasia	451
2.3.3 Alveolar Duct and Alveoli	441	6.4 Mesothelial Hyperplasia	451
2.3.4 Bronchial-Associated Lymphoid Tissue	442	6.5 Alveolar/Bronchiolar Adenoma and Carcinoma	452
2.3.5 Pulmonary Vasculature	442	6.6 Bronchial Adenoma and Carcinoma	455
2.3.6 Pleura and Mediastinum	443	6.7 Squamous Cell Carcinoma	455
2.4 Physiology	443	6.8 Cystic Keratinizing Epithelioma	456
<b>3 Congenital Lesions</b>	<b>443</b>	6.9 Sarcoma	457
<b>4 Infectious Diseases</b>	<b>444</b>	6.10 Malignant Mesothelioma	457
4.1 <i>Mycoplasma pulmonis</i>	444	6.11 Mediastinal Neoplasms	458
4.2 Cilia-Associated Respiratory Bacillus (CAR Bacillus)	444	6.12 Metastatic Neoplasms	458
4.3 <i>Corynebacterium kutscheri</i>	444	<b>7 Miscellaneous Lesions</b>	<b>459</b>
4.4 <i>Pneumocystis carinii</i>	445	7.1 Gavage-Related Lesions	459
4.5 Rat Coronavirus	445	7.2 Hair Embolism	459
4.6 Sendai Virus	445	7.3 Cartilaginous Metaplasia	460
4.7 Rat Polyomavirus	446	7.4 Osseous Metaplasia	460
<b>5 Nonproliferative, Degenerative, and Vascular Lesions</b>	<b>446</b>	7.5 Goblet Cell Metaplasia	460
5.1 Degeneration and Necrosis	446	<b>8 Toxicologic Lesions</b>	<b>460</b>
5.2 Fibrosis	446	8.1 Toxicity of Particles	460
5.3 Alveolar Proteinosis (Lipoproteinosis)	446	8.2 Toxicity of Gases	461
5.4 Alveolar Histiocytosis (Infiltrate Cellular, Histiocyte)	447	8.3 Toxicity of Chemicals Administered Systemically	462
		8.4 Carcinogenesis	462
		<b>References</b>	<b>463</b>

## 1. INTRODUCTION

The lung is constantly exposed to a large volume of inhaled air that may contain toxicant xenobiotics. With the possibility of exposure to a variety of respiratory

toxicants from airborne pollutants in our environment during the course of daily activities, in occupational settings, the use of aerosol sprays for household products, and the development of inhalant bronchial therapies, pulmonary

toxicology has become an important subspecialty of toxicology. The toxic effects caused by inhalation of gases and particles, ingested chemicals can also have profound effects on the lungs. The pulmonary circulation receives the total cardiac blood output and the lungs are susceptible to injury from blood-borne toxicants since the lungs are capable of metabolizing a variety of xenobiotics and may form metabolites that are more or less toxic than the parent compound (Zhang et al., 2006). Similar to the upper respiratory tract, toxicity from air- or blood-borne toxicants is dependent on the physiochemical characteristics and concentration of the toxicant, duration of exposure, site/tissue specific sensitivity, and the integrity of defense mechanisms.

Although the lung is primarily a means for the exchange of carbon dioxide and oxygen, the lung also has some important nonrespiratory metabolic functions, such as the regulation of circulating vasoactive amines and prostaglandins (Joseph et al., 2013). Pathologists need to be cognizant of systemic alterations that can occur secondary to loss of these pulmonary functions.

For toxicologic studies, good gross examination and proper fixation are paramount in the preparation of the lung for histological examination. The usual procedure is intratracheal instillation of formalin fixative (4–6 mL) into the airways followed by ligation of the trachea to maintain the expanded state of the alveoli and immersion in fixative to complete fixation. Instilling an excessive volume of fixative will cause distortion and disruption of alveolar walls, while a less than adequate volume will result in incomplete expansion of the lung. For stereology and morphometric studies, the lung must be fixed under constant pressure—25 cm of water pressure will result in uniform expansion without distortion. The methods for stereology and morphometry are very well defined (Bolender et al., 1993; Weibel et al., 2007). The pathologist must be aware that intratracheal instillation may carry material from the major airways into the alveoli, and displace lung exudates and inflammatory cells thereby masking subtle inflammatory effects—vascular perfusion of fixative is the method of choice if it is important to maintain the mucous layer or determine the precise location of cells and any particulate matter in the airways. Intratracheal instillation may create artifactual changes such as rupture of alveoli that could be misinterpreted as emphysema, or diffusion of fixative into peribronchiolar and perivascular interstitial tissue that may be misinterpreted as edema (Renne et al., 2001).

## 2. NORMAL LUNG

### 2.1. Embryology

The primordium of the respiratory system develops from a diverticulum of the ventral wall of the primitive foregut

with the formation of the tracheobronchial groove (primitive trachea) and two endodermal lung buds which invade the mesoderm and join at the midline to form the primordial lung. The lung buds undergo branching morphogenesis to give rise to the branching tubular primordium of the lung by interacting with the mesoderm (McAteer, 1984; Morse et al., 1979; Yamada et al., 2002). Around embryonic day 13.5, the right lung bud divides into three primitive bronchi, while the left bud stays undivided and forms a single bronchus (Yamada et al., 2002; McAteer, 1984; Morse et al., 1979). Commonly described histological stages in mammalian lung development include the following: (1) Pseudoglandular stage (E13–E18.5) where the epithelial diverticulum from the foregut divide and grow into the surrounding mesenchyme; (2) Canalicular stage (E21–E22) where differentiation of the epithelium of the future gas exchange region occur along with vascularization and angiogenesis; (3) Saccular stage (E23–birth) where the aerated appearance of the lung is evident because of the remodeling and differentiation of alveolar epithelial cells; and (4) Alveolar stage (PND ~4 to ~21) where alveolar formation and maturation occurs (Burri and Moschopoulos, 1992; Warburton et al., 2010; Yamada et al., 2002). Around E17 and E18 the lung is predominantly composed of branching, tubular airways surrounded by mesenchyme. The branching of airways continues on E19 and E20. Around E23 the lung is composed of saccular structures which represent prospective alveolar acini. At birth, the rat lung consists of saccular structures which gradually progresses to mature alveoli by PND 21 (Burri, 1974; Burri and Moschopoulos, 1992).

The new-born rat lung does not have true alveoli, but contains smooth-walled air channels and saccules that correspond to the alveolar ducts and alveolar sacs in the adult (Burri, 1974). The saccules appear morphologically similar to alveoli, but are larger. The majority of alveoli are formed during the first 3 weeks of life with the outgrowth of secondary septa that transform the saccules into the alveolar sacs and alveoli. The lung volume increases about four times as the lung attains its mature structure by 3 weeks of age. During this early postnatal period, the alveolar surface area increases more than fivefold (Vidic and Burri, 1983).

A few mononuclear cells with periodic acid-Schiff (PAS)-positive cytoplasmic granules are found in the stroma of the rat lung by day 14 of gestation. These cells show mitotic activity, increase in number, and some are found on the airway surface by day 16. As fetal development proceeds, these cells begin to resemble macrophages, and by day 3 after birth, those within the alveolar lumens have phagolysosomes and other inclusions typical of alveolar macrophages (Sorokin et al., 1984). The evidence suggests that a resident self-replicating population of macrophages is established at the outset of lung formation.

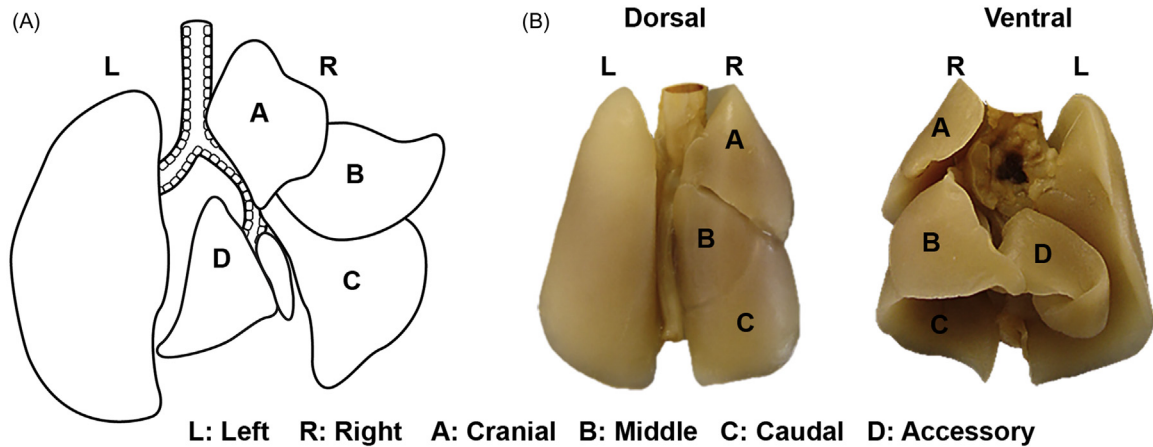


**FIGURE 23.1** Anatomy of the Rat lung. (A) Illustration showing extrapulmonary bronchi entering left and right lung lobes. (B) Gross anatomy showing dorsal and ventral aspects of the lung.

## 2.2. Anatomy

The trachea is a slightly flattened, oval, tubular structure that measures approximately 33–35 mm from its origin at the larynx to the tracheal bifurcation. In the adult rat, the diameter of the trachea is approximately 3 mm horizontally by 1.5–2 mm vertically. The wall is approximately 1 mm thick and is supported by 24 circular cartilages (Hebel and Stromberg, 1976). Proximal to its bifurcation, the trachea dilates and then divides asymmetrically into left and right primary (extrapulmonary) bronchi. The lung has a single left lobe and four right lobes that follow the bifurcations of the bronchial tree (Figure 23.1). Three to 4 mm distally, the right primary bronchus gives rise first to the cranial lobar bronchus, followed by the middle lobar bronchus and the accessory lobar bronchus, and finally terminates as the caudal lobar bronchus. These bronchi conform to the lobes of the right lung, which consist of the anterior (apical or cranial), middle (cardiac), median (azygous or accessory), and posterior (caudal) lobes. The left primary bronchus serves the single large left lobe, and 8 mm distal to the bifurcation, gives rise to a ventral branch and further distally, three dorsolateral, three dorsomedial, and three ventral segmental bronchi arise. Small plates of cartilage support the walls of the extrapulmonary bronchi but are not present in the walls of the intrapulmonary airways.

The bronchus entering each lobe of the lung gives rise successively to smaller secondary bronchi from which the bronchioles originate. In the rat, airway bifurcations generate a major segment at a small angle from the parent airway and a minor segment that arises at a much greater angle. This monopodal asymmetric branching is different from a nearly symmetric dichotomous branching in humans (Pinkerton et al., 2015; Schlesinger and McFadden, 1981). The pattern of branching can affect the

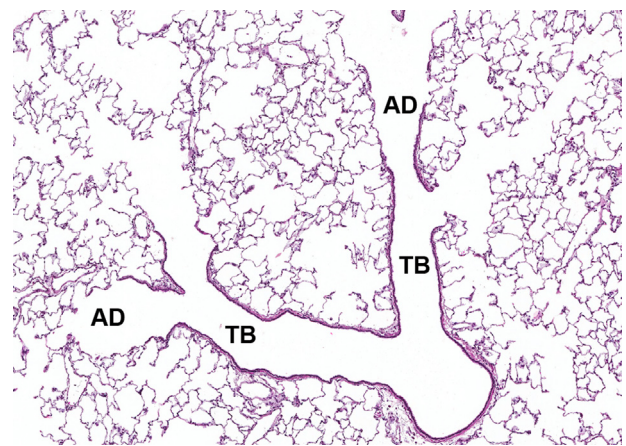


**FIGURE 23.2** Terminal bronchioles (TB) giving rise to the alveolar ducts (A). The alveolar ducts have an average of six generations in the rat.

airflow pattern and particle deposition in the lung (Hofmann et al., 1996; Yeh et al., 1976; Brown, 2015)

The number of airway segments from the bifurcation of the trachea to the terminal bronchiole varies from 13 to 20 depending on the lobe (Yeh et al., 1979). The transition from conducting (bronchioles) to respiratory airways is abrupt, with a short poorly developed respiratory bronchiole giving rise to the pulmonary acinus (Peake and Pinkerton, 2015). The rat lacks the well-developed respiratory bronchiole that is characteristic of primate lungs including those of humans. The pulmonary acinus, which serves as the gas exchange unit, consists of a branching system of alveolar ducts (approximately six generations in the rat) ending blindly in alveolar sacs (Figure 23.2). Alveoli evaginate from the alveolar ducts and alveolar sacs. The average diameter of the alveoli is  $70.2 \pm 7.0$   $\mu$ m. The terminal bronchiole, alveolar ducts, and associated alveoli are often referred to as the centriacinar region of the lung.

The lung has a dual arterial supply with both pulmonary and bronchial arteries (Ferreira et al., 2001; Kay, 2015). The bronchial arteries, considered to be the nutrient artery of the lung, supply the lower half of the trachea, lungs, bronchi, vasa vasorum of pulmonary artery and vein, visceral pleura, and associated lymph nodes. In general, there are two bronchial arteries, left and right, which arise from subclavian artery or its primary branches (Ferreira et al., 2001). The left and right pulmonary arteries from the pulmonary trunk, deliver blood to the lung for gas exchange and to the pleura. The pulmonary artery gives rise to one axial artery for each lobe, which provides larger branches that follow the airways and smaller branches that do not. Arteries following the airways extend to the level of the alveolar ducts (Hislop and Reid, 1978). Bronchial-pulmonary arterial anastomoses occur near the hilum in the rat and rare extrapulmonary anastomoses can occur (Ferreira et al., 2001; McLaughlin, 1983). The pulmonary venous system drains the pleura, alveoli, bronchioles, and most bronchi. The confluence of veins from the pulmonary lobules form pulmonary veins, one from each lobe, that join to form a single pulmonary vein drain into the left auricle (Nakakuki, 1983; Hosoyamada et al., 2010). The bronchial veins drain the trachea, esophagus, lungs, bronchi, and associated lymph nodes and enter the superior vena cava.

The pleura is a thin serous membrane that envelops the lungs (visceral pleura) and lines the thoracic cavity (parietal pleura). These pleurae are continuous at the hilus of the lungs where the pulmonary and bronchial vessels, primary bronchi, nerves, and lymphatics penetrate. The visceral pleura of rats is thin compared to that of humans and large animals (Peake and Pinkerton, 2015). Also, the visceral pleura of rats have sparse lymphatic vessels as opposed to an extensive lymphatic network seen in humans (Leak and Jamuar, 1983). Connective tissue septa branching from the visceral pleura and penetrating the pulmonary parenchyma is very minimal in rats and hence the bronchopulmonary segments are not distinct on the pleural or cut surface (Peake and Pinkerton, 2015).

The mediastinum is the fibrous, loose areolar connective tissue in the center of the thoracic cavity. It lies between the sternum and the vertebral column, and extends from the thoracic inlet, caudally to the diaphragm. It is bounded laterally by the pericardium and the mediastinal pleura, which are continuous with the parietal pleura. The mediastinum separates the left and right lungs and provides flexible support for the tissues and organs of the thoracic cavity. With the exception of the lungs, it supports all of the major tissues of the thoracic cavity including the heart and its great vessels, segments of the trachea and esophagus, the thymus, blood vessels, lymph nodes, lymphatics, and nerves.

## 2.3. Histology

### 2.3.1. Trachea, Bronchi, and Bronchioles

The epithelium of the extrapulmonary airways is pseudostriated columnar whereas that of the intrapulmonary airways is simple columnar. Cell types include ciliated epithelial, nonciliated Club (Clara) cells, mucous (goblet), and serous, neurosecretory, intermediate and brush cells, and basal cells (Marin et al., 1979; Jeffery and Reid, 1975; Dormans, 1983; Alexander et al., 1975). In the rat, the epithelium of the trachea thins distally. There is zonation of ciliated cells in the trachea with cilia rich zones over the tracheal ligaments with fewer ciliated cells over the tracheal cartilages (Oliveira et al., 2003). In the proximal trachea, distal trachea, extrapulmonary bronchus, intrapulmonary bronchus, and bronchioles, approximately 17%, 33%, 35%, 53%, and 65% of cells, respectively, are ciliated (Jeffery and Reid, 1975). The remaining cells are predominantly secretory cells (serous, goblet, or Club cells). Greater details of the cell types and their density are provided in other publications (Reynolds et al., 2015; Plopper and Hyde, 2015). The ciliated cells are important for movement of the mucous blanket (and particulate matter) up the airways and out of the lung.

Club cells are not reported to be present in rat trachea and major bronchi, and are present in the bronchioles (Plopper et al., 1983; Reynolds et al., 2015; Plopper, 1983). Club cells have a distinct morphology characterized by a prominent domed apical bleb that projects above the epithelium and a basal nucleus (Figure 23.3). They can be identified in tissue sections by immunohistochemical staining for their main secretory protein CC10 or Club cell secretory protein (CCSP), a member of the secretoglobulin family of proteins (Singh and Katyal, 2000). Club cells are multifunctional with roles in immune modulation, xenobiotic metabolism, synthesis of

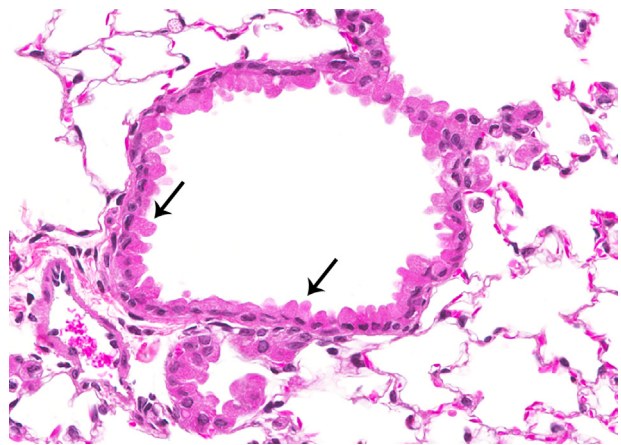


**FIGURE 23.3** Transverse section through a terminal bronchiole shows Club cells with characteristic apical bleb (arrows).

components (surfactant, mucin) of the mucociliary blanket, and as a progenitor cell of the terminally differentiated ciliated cells (Reynolds and Malkinson, 2010). This cell possesses a cytochrome P-450-dependent monooxygenase system (Plopper, 1983) that may be important in the activation of potentially carcinogenic compounds.

Goblet cells are rare in the trachea of rats and occur primarily in the lower trachea and primary bronchi and contain neutral and/or acid glycoproteins—goblet cells constitute less than 1% of the total epithelium in the rat (Jeffery and Reid, 1975; Dormans, 1983). The serous cell is found most frequently in the epithelium of the trachea and main extrapulmonary bronchi and in the glands of the trachea and larynx (Jeffery and Reid, 1975; Dormans, 1983; Plopper et al., 1983).

Neurosecretory or neuroendocrine cells (Kultschitzky cells) are present individually or in very small clusters within the epithelium at all levels of the respiratory tract (Edmondson and Lewis, 1980; Dormans, 1983; Genechten et al., 2004; Adriaensen et al., 2003). Neurosecretory cells are identified ultrastructurally by characteristic electron-dense secretory cytoplasmic granules that contain serotonin, calcitonin, bombesin, and enkephalin (Adriaensen et al., 2003). Immunohistochemical staining with Protein G product 9.5 (PGP 9.5), calcitonin gene-related peptide, synaptophysin and synaptic vesicle protein-2 has been used to identify pulmonary neurosecretory cells (Pan et al., 2014; Adriaensen et al., 2003). Aggregates of approximately 10–20 of these cells are found at bronchiolar bifurcations and are known as neuroepithelial bodies (NEB) (Gosney and Sissons, 1985). They are sometimes associated with unmyelinated axons and are thought to function as chemoreceptors. The NEB are sensitive to oxygen tension in the inspired air, and hypoxia will cause degranulation of the cells (Adriaensen et al., 2003; Haworth et al., 2007).

Basal cells are found at the base of the epithelial cell layer. They may be stem cells or progenitor cells for the tracheobronchiolar epithelium with a cell turnover time of about 20–30 days. While the cells are present in trachea and bronchi, they are in very low numbers or absent in the terminal bronchioles (Jeffery and Reid, 1975; Dormans, 1983; Mercer et al., 1994).

Tubuloacinar, serous glands are located in the submucosa of the trachea. The glands are present predominantly in the intercartilagenous submucosa on the ventral aspect and their density decreases towards the bronchial bifurcation. There is some strain variability in the distribution of glands as Sprague-Dawley and Brown Norway rats have submucosal glands throughout, whereas F344 rats have none in the lower trachea and bronchi (Widdicombe et al., 2001; Ohtsuka et al., 1997; Spicer et al., 1982). The tracheal epithelium is supported by fibrous connective tissue, smooth muscle, and cartilage rings, but the rings disappear soon after the airways enter the lung.

### 2.3.2. Terminal Bronchioles

The terminal bronchioles are lined by simple cuboidal epithelium consisting primarily of Club cells (37%) and ciliated cells (55%). About 8% of the terminal bronchiole lining cells do not fit either category. The terminal bronchioles lack goblet cells and the protective mucous blanket, which in part may explain the unique sensitivity of this airway to inhaled oxidant gases such as ozone (Plopper and Hyde, 2015; Evans et al., 1976; Lum et al., 1978; Schwartz, 1986).

### 2.3.3. Alveolar Duct and Alveoli

The functional or gas exchange unit of the lung consists of an alveolar duct and its associated alveolar sacs and alveoli. The alveolar epithelium consists primarily of Type I and Type II pneumocytes. Although the total numbers of Type I and Type II cells are nearly equal, the Type I cells, because of their greater surface area, cover over 95% of the alveolar surface (Pinkerton et al., 1982; Dormans, 1983). Type II cells are located primarily in recesses in the corners of the alveoli. Type II cells are the progenitors of Type I cells and are the source of the surfactant that is found in the alveoli (Adamson and Bowden, 1975; Schwartz, 1986). Type II cells have characteristic lamellar bodies which contain the phospholipid-rich pulmonary surfactant that is found on the surface of the alveoli and is needed to maintain surface tension. The lamellar bodies are secreted onto the alveolar surface (Dormans, 1983).

Another type of cell, the alveolar brush cell has been recognized in the alveoli. The surface of this cell is covered with short microvilli and the cytoplasm contains fine filaments. The function of this cell is not known, but it may be concerned with stretch or chemoreception (Meyrick and Reid, 1968; Chang et al., 1986; Reid et al., 2005).

Pulmonary macrophages are located on the surface of the alveoli and within the alveolar interstitium. Alveolar macrophages represent approximately 3–5% of all cells in a normal lung and function as antigen presenting cells and as regulators of host defense and lung homeostasis (Laskin et al., 2011, 2015). Under normal conditions in the rat, the alveolar macrophage can proliferate to maintain and replenish the normal pulmonary macrophage population (Shellito et al., 1987). During the first week of life, alveolar macrophages develop from fetal monocytes which differentiate into long-lived cells in response to an instructive signal provided by granulocyte macrophage colony-stimulating factor (GM-CSF) (Guilliams et al., 2013). The extent to which blood monocytes contribute to this stable population of alveolar macrophages is uncertain (Shellito et al., 1987). In inflammatory conditions, circulating monocytes arising from the bone marrow also

serve as a source of alveolar macrophages (Misharin et al., 2017). It is estimated that more than 1 million macrophages are cleared from the lung to the oropharynx hourly (Spritzer et al., 1968), thus serving as an important mechanism for clearance of particulate matter from the lung.

Interstitial macrophages are present in the interstitial spaces of the alveolar septa and constitute approximately 2% of the lung cell population (Lehnert et al., 1985). Some morphological and functional similarities and differences between interstitial and alveolar macrophages have been described (Laskin et al., 2015).

### 2.3.4. Bronchial-Associated Lymphoid Tissue

Bronchial-associated lymphoid tissue (BALT) is considered part of the mucosa-associated immune system and is present in rats (Pabst and Gehrke, 1990; Bienenstock and McDermott, 2005). It consists of focal aggregates of lymphocytes located in the submucosal of the bronchial wall primarily at branching of the airways (Figure 23.4) (Cesta, 2006). In contrast to the gut-associated lymphoid tissue (GALT), in which the majority of lymphocytes in Peyer's patches are B-lymphocytes, those in BALT are predominantly T-lymphocytes (Crawford and Miller, 1984, Otsuki et al., 1989). The modified epithelial cells overlying BALT have apical microvilli that function to increase the surface area for antigen sampling (Sminia et al., 1990).

### 2.3.5. Pulmonary Vasculature

The pulmonary trunk gives rise to right and left pulmonary arteries. Each lobe has one single axial artery from which the branches arise (Hislop and Reid, 1978). Two types of arteries branch from the axial artery to supply

each lobe. One type arises at an acute angle and the second type branches at a right angle from the axial artery (Lane et al., 1983). Morphologically, the two types of vessels differ with respect to their muscular layers. At the hilum of the lung the tunica media of the pulmonary artery consists of a circumferentially arranged layer of smooth muscle bounded by internal and external elastic laminae. Some arteries have an oblique muscle layer external to the external elastic lamina and the circular muscular layer. The oblique muscle layer makes the vessel wall appear unusually thick relative to the diameter of the lumen and has been mistaken for medial hypertrophy. As these arteries decrease in size, the circular muscle layer ends, but the oblique muscle layer continues as a discrete spiral bundle (Figure 23.5). On cross-section, the vessel may appear to have an irregularly thickened muscle. Eventually the arterial branches become nonmuscular, usually at the level of the alveolar duct. The function of this oblique muscle segment is not known (Meyrick et al., 1978).

In the rat lung, veins of all sizes have an internal sub-endothelial thin layer of smooth muscle and an external layer of striated cardiac muscle which is continuous with the myocardium of the left atrium (Figure 23.6). The cardiac muscle around the pulmonary vein is arranged as an internal circular layer and an external longitudinal layer. There is great variation in the number of layers of cardiac muscle around the pulmonary vein. The external longitudinal layers extend further than the circular muscle layer. The cardiac muscle is present in the axial vein and its primary branches closer to the hilum. As the pulmonary vein branch and go deeper, they lose cardiac muscle layer (Almeida et al., 1975; Hosoyamada et al., 2010). Disease processes that affect cardiac muscle can affect that of the pulmonary veins as well. With acute myocarditis, for

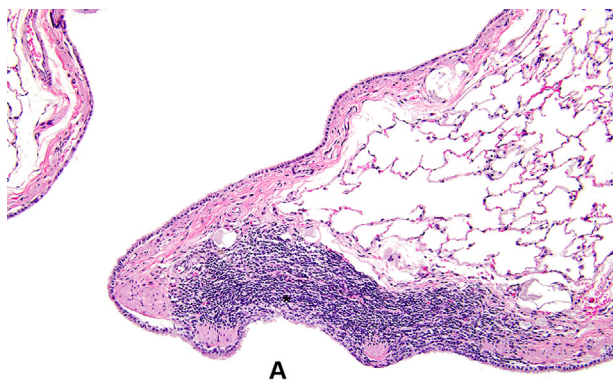


**FIGURE 23.4** Bronchiole-associated lymphoid tissue (asterisk) adjacent to the airway (A).

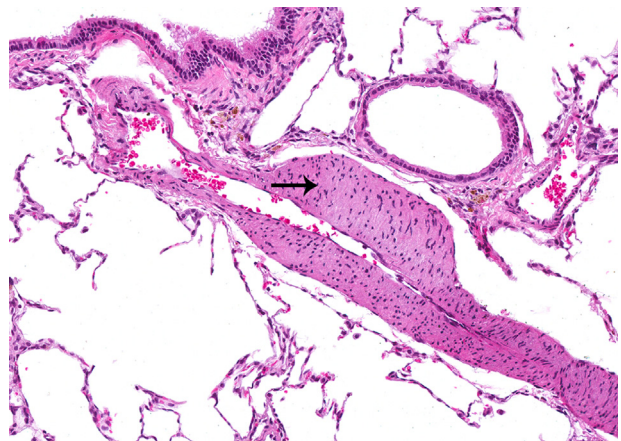


**FIGURE 23.5** External oblique muscle (arrow) surrounding a right-angle branch artery. This is a unique feature of the rat pulmonary vasculature.

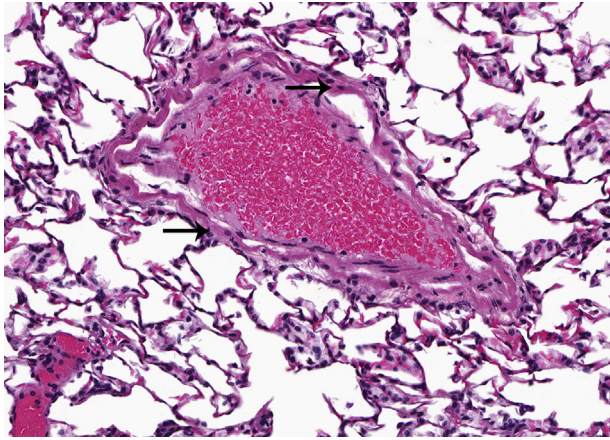


**FIGURE 23.6** Myocardial cells (arrows) surrounding a pulmonary vein.

example, there may also be inflammation of the cardiac muscle in the pulmonary veins.

The lung contains both lymphatic capillaries and collecting lymphatic vessels. As in other tissues, lymphatic capillaries are thin-walled vessels located in areas where there is abundant connective tissue. They are present in the pleura and the interlobular and connective tissue surrounding terminal and respiratory bronchioles, pulmonary arterioles and pulmonary venules. Compared to lymphatic capillaries, collecting lymphatic vessels have a larger diameter, are thicker, are more numerous, and have valves. Collecting lymphatics drain toward the hilum where they empty into lymph nodes (Leak and Jamuar, 1983; Leak, 1980).

### 2.3.6. Pleura and Mediastinum

There are two types of pleural membranes. The visceral pleura is closely applied to the surface of the lungs and consists of a single layer of squamous to low cuboidal mesothelial cells that have surface microvilli. The mesothelial cells sit on a thin basement membrane of thin layer of loose collagenous fibrous tissue that beneath which is a thicker layer of dense fibroelastic tissue. Beneath the visceral pleura there is a vascular layer of capillaries and lymphatics. The parietal pleura is thicker and less elastic layer that lines the thoracic cavity. The mediastinum consists of a mixture of collagen, reticular and elastic fibers, and adipose tissue that loosely surround and fills the spaces between the tissues and organs it encompasses.

The mediastinum consists of a mixture of collagen, reticular and elastic fibers, and adipose tissue that loosely surround and fill the spaces between the tissues and organs of the thoracic cavity.

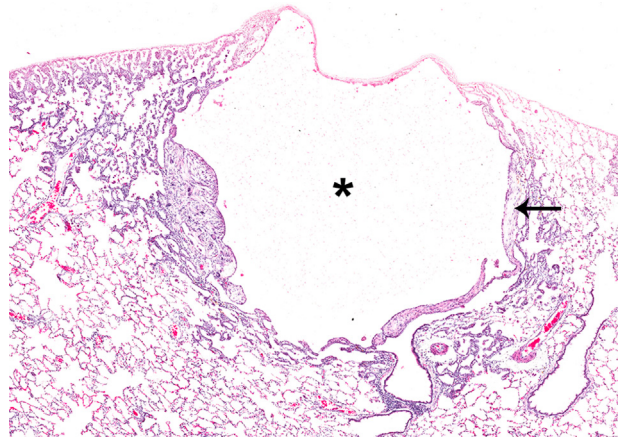


**FIGURE 23.7** Subpleural cyst (asterisk) with mild fibrosis (arrow) in the cyst wall.

## 2.4. Physiology

The lung has major metabolic functions including activation of angiotensin and inactivation of bradykinin, serotonin, norepinephrine, and certain prostaglandins. The lung also synthesizes and releases a variety of biologically active compounds including amines, peptides, complement, prostaglandins, arachidonate metabolites, and other lipids such as platelet activating factor (de Wet and Moss, 1998; Touya et al., 1986). A discussion of the metabolic functions of the lung is beyond the scope of this chapter, but the pathologist needs to be cognizant that metabolic events in the lung will be altered in severe pulmonary disorders. Thus, pulmonary injury may result in systemic responses subsequent to metabolic disorders in the lung.

## 3. CONGENITAL LESIONS

Congenital lesions of the lung are rare. Simple cysts are an incidental finding (Figure 23.7). They may be subpleural, cause minimal compression of the adjacent parenchyma, and have some fibrosis in the wall. Frequently they do not have a distinct epithelial cell layer in the wall and are lined by fibrous tissue. It is not known whether these lesions are present from birth or whether they arise later as a result of airway obstruction. The latter would not be considered congenital lesions.

Hypoplasia of the lung parenchyma is a rarely observed lesion in neonatal rats. This lesion is characterized by decreased total lung size and lung tissue volume, retarded development of the alveoli. Alveolar Type II pneumocyte development is not affected but the differentiation of Type II pneumocyte to alveolar Type I pneumocyte is probably affected. Lung hypoplasia has been

induced by exposure of pregnant dams to the herbicide Nitrofen and has been used as an animal model for human pulmonary hypoplasia (Guilbert et al., 2000; Brandsma et al., 1994).

## 4. INFECTIOUS DISEASES

Generally, few infectious-related inflammatory lesions are seen in the lungs of F344 rats bred and maintained under barrier conditions for use in toxicology studies. Current laboratory animal management practices within rodent facilities are such that spontaneous infectious processes should be infrequently encountered.

Bacteria and viruses can cause necrosis and inflammation in the lungs of rats. These lesions are important because they can affect the pulmonary response to toxic agents. Clearance of particulate matter from the lung may be dramatically decreased if there is necrosis of ciliated cells in the airways or alterations in the mucous blanket, resulting in the retention of particles in the lung. The rate of cell turnover may be increased, which has the potential to affect the response to a carcinogen. Morphological changes induced by infectious agents may also mask a toxic effect, and thus subtle chemical-related changes may be missed. The pathology caused by few of the more relevant infectious agents that have been associated with pulmonary disease in experimental studies is discussed below. The reader is referred to publications on laboratory rodents for a more complete discussion of the infectious diseases that affect the respiratory tract of rats (Otto et al., 2015; Barthold et al., 2016).

### 4.1. *Mycoplasma pulmonis*

Pulmonary infection due to *Mycoplasma pulmonis* (*M. pulmonis*) has the potential to interfere with a wide variety of toxicology studies in rats, particularly inhalation studies since the respiratory tract is the primary target. However, with improved animal quality and better animal husbandry, *M. pulmonis* now rarely complicates toxicology studies. *M. pulmonis* infection compromises the immune system and predisposes to secondary respiratory bacterial and viral infections such as CAR bacillus and Sendai virus. The organism has a predilection for the epithelial cells of the respiratory tract, middle ear, and the female reproductive tract. Infection may begin in young rats and is usually clinically silent. Clinical signs are primarily observed in older rats and are nonspecific and include rales and dyspnea, snuffle and chattering, ocular and nasal discharges, chromodacryorrhea, rubbing of the eyes, and head tilt (Otto et al., 2015). Rats with severe middle ear involvement may spin when held up by the tail. Gross lesions of *M. pulmonis* infection include serous to suppurative inflammation in the upper respiratory tract

(nasal cavity, larynx, and trachea), lung, and middle ear (Barthold et al., 2016). In the lung, there is often atelectasis, bronchiectasis, and abscesses that in adults with end stage disease, lead to the “cobblestone” appearance of the lung. Affected lobes are cranioventral in distribution and may be unilateral or bi-lateral and plum-colored. The tympanic bullae may contain serous to inspissated purulent material.

Histologically, respiratory tract lesions consist of accumulation of neutrophils within the lumina of the nasal cavity, eustachian tubes, middle ears, trachea, and airways of the lung. There is prominent suppurative to mononuclear cell (lymphocyte and plasma cell) inflammation in the submucosa of affected tissues and lung parenchyma. Inflammation is accompanied by prominent hyperplasia (often pseudoglandular) and squamous metaplasia of the nasal epithelia, and hyperplasia of the peribronchial and peribronchiolar alveolar epithelium Type II cells. Within the lumina of the bronchi and bronchioles, mucin and neutrophil exudation increases during the course of the disease to the point of bronchiectasis with the formation of abscesses. A consistent and prominent lesion in the lung is marked peribronchial, peribronchiolar hyperplasia (cuffing) in the BALT. Frequently, perivascular lymphocyte hyperplasia becomes massive and can be confused with malignant lymphoma (Schoeb et al., 2009a,b).

### 4.2. Cilia-Associated Respiratory Bacillus (CAR Bacillus)

A bacillus associated with the cilia of the respiratory epithelium has been found in a few toxicology studies. This bacillus does not grow on conventional media, but can be demonstrated between the cilia of respiratory epithelium by silver stains or by electron microscopy. The bacteria has been now identified as *Filobacterium rodentium* (Ike et al., 2016). In rats, infection is usually asymptomatic although nonspecific clinical signs, such as weight loss and dyspnea may be observed (Otto et al., 2015). Gross lesions are often not present but coinfection with *M. pulmonis* and other pathogens may occur, resulting in suppurative inflammation. Infection causes peribronchial and peribronchiolar mononuclear inflammatory cell inflammation. Warthin–Starry or methenamine silver staining will reveal filamentous bacilli among cilia of respiratory epithelium from the nasal to the bronchiolar epithelia (Barthold et al., 2016; Otto et al., 2015).

### 4.3. *Corynebacterium kutscheri*

*Corynebacterium kutscheri* is a gram-positive bacterium that can affect rats and other laboratory animals. Infection with this organism is rare, and when affected, rats will have nonspecific clinical signs. Grossly, multiple

randomly distributed abscess due to septic emboli are present in lungs and other organs. Histologically, in the abscessed areas, granulomatous inflammation can be present (Otto et al., 2015; Barthold et al., 2016).

#### 4.4. *Pneumocystis carinii*

Although improved animal care and husbandry have eliminated most infectious agents, *Pneumocystis carinii* (*P. carinii*), a fungal organism (Stringer, 1993), may latently infect rats and spontaneous cases are occasionally observed in experimental rats. The fungus causes a host-specific infection presenting as two distinct disease syndromes in immunocompromised and immunocompetent rats. Infection may be fatal in neonates. With exposure to chemicals with immunosuppressive properties, evidence of *P. carinii* infection may be observed. In immunocompromised rats, *P. carinii* proliferates uncontrolled in the lung, causing dyspnea, weight loss, and death. Histologically, the organism appears as abundant foamy material and debris filling the alveoli accompanied by interstitial and perivascular lymphocytic infiltrates. In clinically normal immunocompetent rats, *P. carinii* causes a self-limiting inflammatory lung disease. Gross pulmonary lesions of *P. carinii* infection are visible in 50% or more of infected rats 4–5 weeks after infection, and appear as 1–4 mm gray, flat to raised lesions randomly distributed throughout all lung lobes. These lesions will usually resolve after another 8–12 weeks. Characteristic histologic lung lesions consist of mild to severe multifocal perivascular infiltrates of lymphocytes, plasma cells, and macrophages and thickening of the alveolar septa by mild to severe lymphohistiocytic infiltrates (Figure 23.8). Multinucleated giant cells may sometimes be present. There may be marked Type II pneumocyte hyperplasia

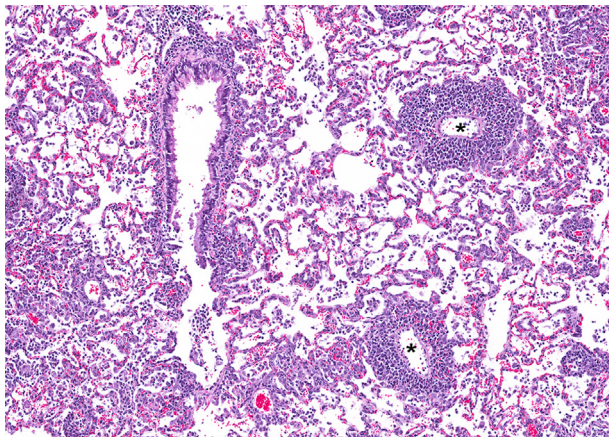


**FIGURE 23.8** Infiltrates of lymphocytes, plasma cells, and macrophages in the rat lung infected with *Pneumocystis carinii*. Note characteristic dense perivascular (asterisks) accumulation of the infiltrating cells.

and interstitial fibrosis in areas of the interstitial infiltrates. After some time, infiltrates in the septa and alveoli are resolved. However, perivascular lymphocyte infiltration persists. Historically, these changes have been attributed to rat respiratory virus (Livingston et al., 2011; Henderson et al., 2012; Kim et al., 2014). Histologically, silver stains such as Gomori's methenamine silver (GMS) can be used to demonstrate the organism within the alveoli. However, fungi cannot be demonstrated in all cases (Livingston et al., 2011). Diagnosis can be confirmed by performing PCR on lung tissue, and infection detected by serological surveillance and monitoring of immunocompetent animals (Henderson et al., 2012). Because *P. carinii* infection causes significant lung inflammation, it can be a confounding factor in inhalation studies, and should be considered when unexpected lymphohistiocytic inflammatory lesions are observed in the lungs of rats.

#### 4.5. Rat Coronavirus

Parker's rat coronavirus (PRC) and sialodacryoadenitis virus (SDAV) were the two coronaviruses most commonly isolated in rats and are now rare to absent in rat colonies. Both have been shown to be capable of producing lesions in the lungs. In the acute phase, there is multifocal necrosis of the respiratory epithelium in the larynx, trachea, bronchi, and bronchioles with edema and an infiltrate of neutrophils and mononuclear inflammatory cells. Alveolar ducts and alveoli surrounding the terminal bronchioles are also affected. An inflammatory exudate consisting of neutrophils and alveolar macrophages is present in the alveolar lumens, and the alveolar walls are slightly thickened due to edema and an infiltrate of leukocytes in the interstitium (Otto et al., 2015; Barthold et al., 2016).

#### 4.6. Sendai Virus

Sendai virus is an RNA paramyxovirus that commonly infects rodents not raised under barrier conditions with modern husbandry practices. In the past, many of the Sendai virus infections in rats were complicated by concomitant infection with *M. pulmonis*. Clinical disease and respiratory tract lesions in rats have rarely been attributed to Sendai virus alone and the virus is seldom detected serologically. Respiratory tract lesions include mild to moderate chronic active inflammation in the nasal cavity with focal to diffuse epithelial necrosis. In the lung, there is focal alveolar and multifocal peribronchial and peribronchiolar chronic active inflammation that resolves in 3–5 days. The presence of virus in bronchial, bronchiolar, and alveolar epithelium is followed by necrosis of the epithelium with regeneration and inflammation. In resolving stages, there is prominent lymphocyte and plasma cell

peribronchial and peribronchiolar cuffing with mononuclear cell infiltrates in the alveolar septa that may persist for several weeks (Barthold et al., 2016). The damage to the respiratory epithelium of airways has the potential to interfere with particle clearance and severely compromise inhalation studies. Since Sendai virus may interfere with the pulmonary immune response and increase the rate of cell replication, especially in the small airways, this viral infection also has the potential to interfere with toxicological studies of chemicals given by other routes as well.

#### 4.7. Rat Polyomavirus

A novel polyoma virus, *Rattus Norvegicus Polyomavirus 2* has recently been described to cause pathology in immunodeficient rats. Although major pathological changes are in submandibular, sublingual and parotid salivary glands, exorbital lacrimal glands, Harderian glands, thyroid, and prostate, intranuclear inclusions can be present in the bronchiolar epithelium and pneumocytes (Besch-Williford et al., 2017).

### 5. NONPROLIFERATIVE, DEGENERATIVE, AND VASCULAR LESIONS

#### 5.1. Degeneration and Necrosis

Degenerative changes in the bronchial, bronchiolar, and alveolar epithelia resulting from exposure to toxic or irritant compounds are similar to those that occur in the upper respiratory tract. Epithelial changes include rounding of the normally cuboidal or columnar epithelial cells with loss of cilia and loss of apical blebs from Club cells. The cytoplasm of degenerating cell may appear clear or vacuolated. The airway epithelium may appear irregular and disorganized. Depending on the nature of the toxicant or irritant and length of exposure, variable necrosis may occur and frequently accompanies degeneration and manifests as karyorrhexis of the epithelial cell with sloughing and loss of the epithelium (Figure 23.9). Necrosis is usually accompanied by variable inflammation, and regenerative and metaplastic epithelial changes may also be evident.

#### 5.2. Fibrosis

Fibrosis of the pleura or alveolar parenchyma including the bronchioles is an infrequent spontaneous finding in laboratory rats (Figure 23.10), but in these sites, is a common response to repeated or chronic injury resulting from infectious disease, systemic administration of chemicals, or inhalation of irritant chemicals. However, severe acute lung injury from a single exposure to highly irritant chemicals may induce a rapid fibrogenic response that may or may not be reversible (Renne et al., 2009). Critical to

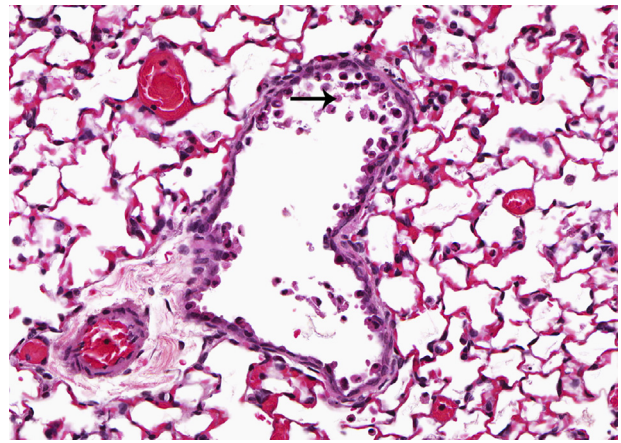


**FIGURE 23.9** Bronchiolar epithelial necrosis characterized by pyknosis, karyorrhexis and sloughing, and loss of epithelium (arrow)

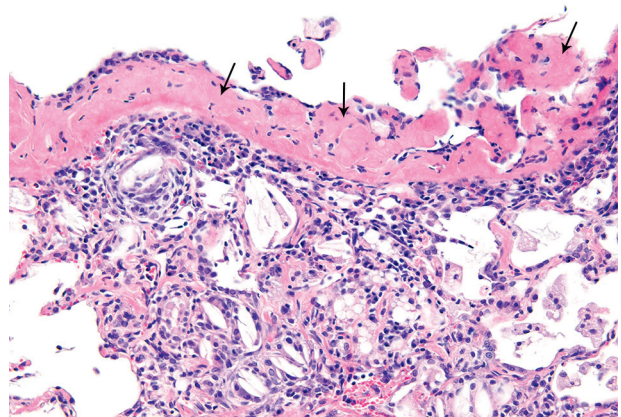


**FIGURE 23.10** Pleural fibrosis (arrows) adjacent to an area of subpleural chronic inflammation in the lung of rat exposed to particulate by inflammation. Note fibrous thickening of the alveolar interstitium within the area of inflammation.

the development of fibrosis is the release of fibrogenic cytokines and fibronectin from pulmonary macrophages activated during the inflammatory response. Fibroblasts migrate into the fibrin casts and produce collagen. Depending on the extent and severity of injury, fibrosis may resolve slowly or may not completely resolve. Chronic exposure of rats to 2,3-butanedione (Morgan et al., 2016), cobalt sulfate heptahydrate (Bucher, 1991), indium phosphide (NTP, 2001), nickel sulfate hexahydrate (NTP, 1996b), and ozone (NTP, 1994) by inhalation has been reported to induce fibrosis.

#### 5.3. Alveolar Proteinosis (Lipoproteinosis)

Alveolar proteinosis is characterized by accumulation of a deeply staining, eosinophilic, amorphous, acellular material within the alveolar lumens (Figure 23.11). Small numbers of alveoli or an entire lobe may be affected.

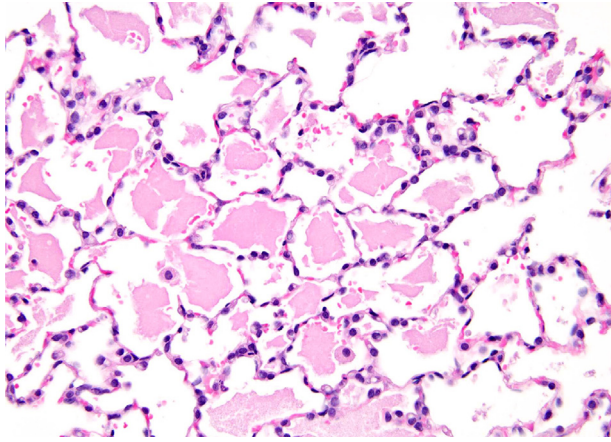


**FIGURE 23.11** Alveolar proteinosis with amorphous eosinophilic material within the alveoli.

There may be little or no associated inflammation, but alveolar macrophages may be more abundant and the alveolar lining cells are more prominent than normal. Although, it is referred to as alveolar proteinosis, the composition of the acellular material is shown to be lipoprotein, rich in phospholipid and serum protein (Bomhard, 2017; Seymour and Presneill, 2002; Hook, 1991; Renne et al., 2009). In humans, alteration in surfactant production and degradation are considered to be the possible causes, and similar mechanism is considered to be involved in rats experimentally exposed to quartz (Seymour and Presneill, 2002; Bomhard, 2017; Hook, 1991). At the molecular level, GM-CSF has been shown to play a critical role (Seymour and Presneill, 2002). Increased surfactant production associated with Type II cell hypertrophy and hyperplasia has been demonstrated in these conditions (Porter et al., 2001; Hook, 1991). It has also been postulated that the dust accumulates in the alveolar macrophages and interferes with the normal clearance of the surfactant produced by Type II cells. In humans, defective macrophage function is also thought to lead to this condition. Granular eosinophilic proteinaceous concretions associated with inflammation have been seen in the lungs of rats inhaling cobalt sulfate. Exposure to cobalt, cobalt sulfate heptahydrate (Bucher, 1991), gallium arsenide (NTP, 2000), indium phosphide (NTP, 2001), metal working fluids, nickel subsulfide (NTP, 1996a), nickel sulfate hexahydrate (NTP, 1996b), aluminum, silicon dioxide, silica, quartz, and titanium dioxide by inhalation has been reported to result in alveolar proteinosis (Bomhard, 2017).

#### 5.4. Alveolar Histiocytosis (Infiltrate Cellular, Histiocyte)

Alveolar histiocytosis is a common incidental finding in older rats and consists of small focal intraalveolar

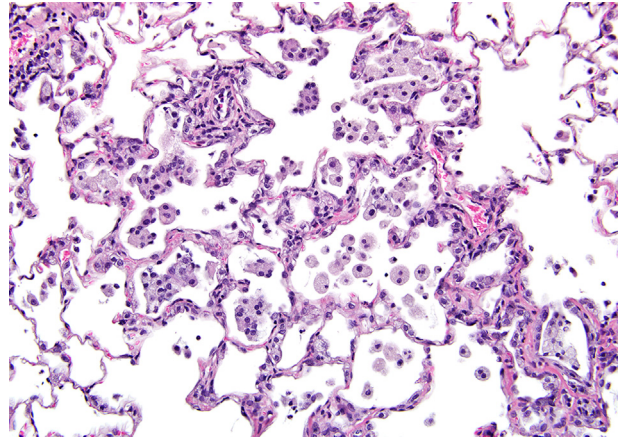


**FIGURE 23.12** Alveolar histiocytosis consisting of macrophages with foamy cytoplasm within the alveoli.

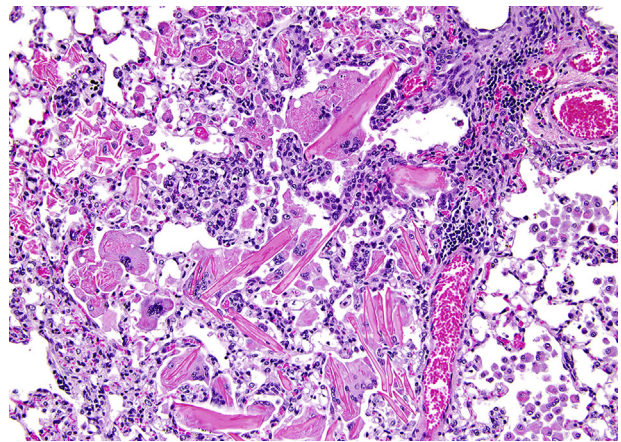


**FIGURE 23.13** Following inhalation exposure to particulates where there is marked proteinosis, the alveolar macrophages may contain intracytoplasmic crystalline material.

collections of alveolar macrophages with abundant foamy (lipid-containing) cytoplasm. These infiltrates are often subpleural or located in the more peripheral regions of the lung and may be accompanied by variable Type II cells proliferation (Figures 23.12 and 23.13), and occasionally perivascular infiltrates of lymphocytes or cholesterol clefts are present. There may also be an increase in surfactant and phospholipid material in the alveoli similar to that in alveolar proteinosis. In inhalation studies, alveolar histiocytosis is a common response to exposure to relatively high concentrations of poorly soluble or insoluble materials, particularly particulates, where deposition exceeds clearance by the lung clearance mechanisms. In these studies, the response may be simple and limited to accumulation of only macrophages within the alveoli, but more frequently, the infiltrates accompany variable Type II pneumocyte hyperplasia and pulmonary inflammation and tissue injury with infiltrates of neutrophils,

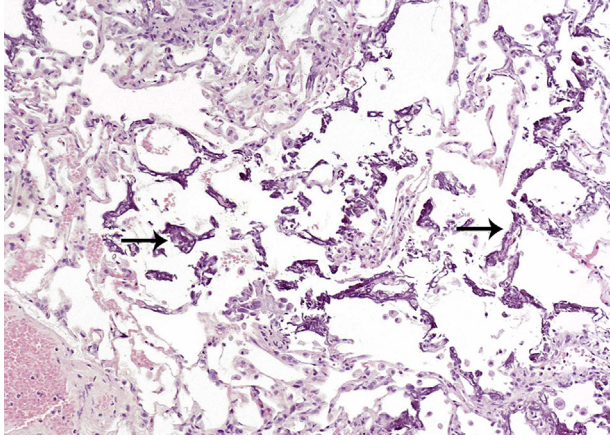


**FIGURE 23.14** Mineralization of the alveolar septa (arrows).

lymphocytes and cholesterol cleft formation and fibrosis. The infiltrating macrophages are generally hypertrophic with a foamy or hypereosinophilic cytoplasmic appearance and may contain eosinophilic crystalline material.

### 5.5. Mineral

Spontaneous mineral (calcium) deposits can occur in the lungs of aged rats with severe chronic end-stage renal disease (Figure 23.14). The deposits appear as irregular, linear, basophilic concretions along the basement membrane of the alveolar septa and the intima and media of small blood vessels. Increased numbers of macrophages may be associated with the mineral deposits.

### 5.6. Pigments

Lung pigment is frequently observed in untreated and treated rats, and as an age-related change or in association with hemorrhage and inflammatory lesions. The most frequently observed lung pigment is hemosiderin, a brown, iron-positive pigment usually found within perivascular or peribronchiolar alveolar macrophages in untreated rats (Figure 23.15). In treated rats, hemosiderin pigment may also be found in alveolar macrophages or free in the alveoli usually associated with areas of chronic alveolar injury, necrosis, inflammation, and hemorrhage, and may also be present in proliferative epithelium that may be associated with these lesions. Lipofuscin may also be found within alveolar macrophages. Inert materials such as corn oil accidentally instilled into the lung during gavage procedures, may also be visible in the lung (Elmore et al., 2014).

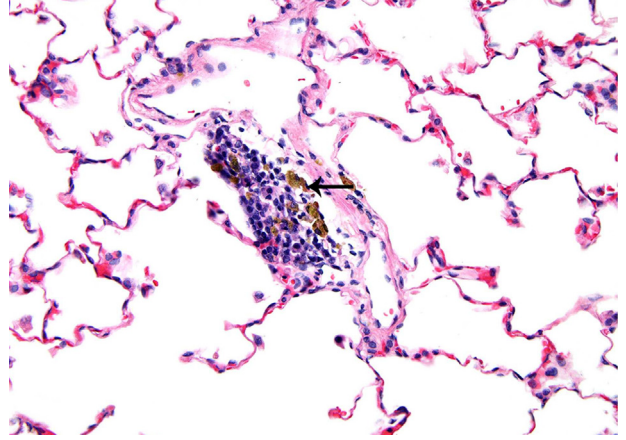


**FIGURE 23.15** Hemosiderin pigment (arrow) in the lung appears as golden yellow material within macrophages in an area of mononuclear cell infiltration.

### 5.7. Inflammatory Lesions

Pulmonary inflammation resulting from exposure to infectious agents, inhalation exposure to injurious chemicals and compounds may occur around the terminal bronchioles and alveolar ducts, and/or within the alveolar parenchyma. In toxicology studies, the inflammatory response may be directly related to the nature and concentration of the inhaled toxicant, site of contact or deposition within the lung, the duration of exposure, the fragility of the epithelium, and type of injury that results. The primary pattern of inflammation is usually bronchiolar/alveolar because the epithelium of the terminal bronchioles, alveolar ducts and adjacent alveoli are sites of initial and maximum contact for vapors and aerosols, and/or deposition of particulate agents. Inhalation of mildly toxic vapors or particulates may cause a transient serous, fibrinous, or suppurative exudate with variable numbers of neutrophils. Inhalation of highly toxic or irritant agents that elicit acute epithelial damage such as ulceration and necrosis results in an acute response that varies from minimal to mild neutrophilic infiltration to suppurative inflammation composed predominantly of neutrophils.

## 6. NONNEOPLASTIC AND NEOPLASTIC PROLIFERATIVE LESIONS

Toxicologically relevant proliferative lesions of the lung typically result from exposure to potentially toxic test materials. Cellular injury that occurs from repeated or chronic exposure to toxicants or irritants induces reparative processes in which the damaged tissue may proliferate (hyperplasia) and/or undergo metaplasia to a different, more resistant cell type, if return to normal morphology is

not complete. Chronic damage and repair (hyperplasia) may result in genetic alterations/mutations that fuel tumorigenesis. The site of these morphologic changes in the lung is heavily dependent upon the nature of the toxicant and the length of exposure.

Proliferative epithelial lesions of the lungs comprise a multistage, morphologic and biologic continuum that consists of focal hyperplasia (that may represent an early stage in the development of neoplasms), adenoma and carcinoma. Because of this continuum, it is sometimes difficult to clearly distinguish between hyperplasia considered preneoplastic and adenomas, or adenomas and carcinomas, and the distinctions may be sometimes arbitrary. In addition, it may also be difficult to separate these neoplasms based on histologic type. In light of such difficulties, by convention, neoplasms originating in the alveolar and/or bronchiolar region of the lung are designated alveolar/bronchiolar adenomas or carcinomas as in the mouse.

Primary pulmonary neoplasms may be of epithelial or mesenchymal origin, and originate in the lung parenchyma and airways. Alveolar/bronchiolar adenomas and carcinomas (including variants with squamous and mucinous cell differentiation) are the most common spontaneous and chemically induced lung tumors in rats (Dixon and Maronpot, 1991; Dixon et al., 2008). The origin of alveolar/bronchiolar neoplasms in the rat has not been as thoroughly investigated. Based on the available literature, chemically induced and naturally occurring neoplasms appear to consist mostly of Type II cells sometimes mixed with low numbers of Club cells. Ultrastructurally, alveolar/bronchiolar neoplasms contain cytoplasmic osmiophilic lamellar inclusions characteristic of Type II pneumocytes (Herbert et al., 1994; Ohshima et al., 1985; Reznik-Schuller and Reznik, 1982; Rehm, 1996; Boorman and Herbert, 1996).

Spontaneous neoplasms of the lung occur at relatively low incidence rates in F344 rats: 2–3% in males and slightly over 1% in females. Spontaneous neoplasms are primarily alveolar/bronchiolar adenoma (0–6% in males; 0–8% in females) or carcinoma (0–6% in males; 0–2% in females). Other lung neoplasms such as squamous cell carcinomas, cystic keratinizing epitheliomas (CKE), and primary spontaneous neoplasms of the bronchial epithelium are rarely observed.

### 6.1. Regenerative Hyperplasia

Regenerative hyperplasia of the airway epithelium or of the alveolar Type II pneumocytes is a common response to injury. The sequelae to repair of degeneration and necrosis of the epithelium of the bronchi, bronchioles, alveolar ducts, and alveoli are generally similar to those described for the upper respiratory tract. Following

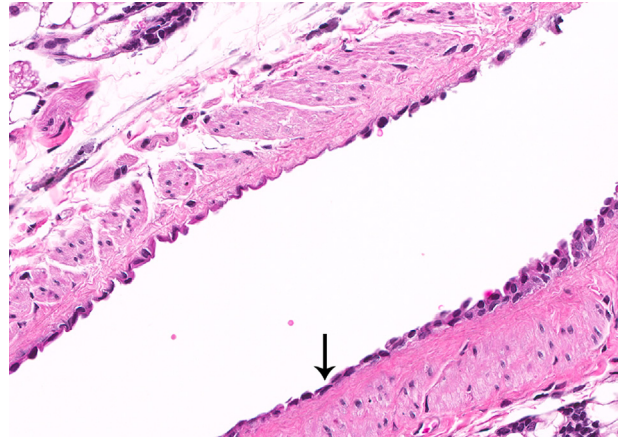


**FIGURE 23.16** Regeneration of the bronchiolar epithelium. Note flattened epithelium lining the airway (arrow).

necrosis of the airway epithelium, the denuded airway surface is re-epithelialized by proliferation of basal cells and/or nonciliated cells at the margins of the lesion. Depending on when the lesion is observed relative to the time of injury, the degree and duration of injury and the relative rates of cell loss and proliferation, one of several different morphological changes is seen. The regenerating epithelium first consists of flattened cells with round to oval nuclei and slightly basophilic cytoplasm (Figure 23.16). If the injury is not prolonged, the regenerating cells rapidly become cuboidal and differentiate into ciliated or nonciliated cells. If there is continued injury and cell loss, differentiation does not occur and the epithelium may become pseudostratified or stratified with one to three layers of undifferentiated cells that are irregular in shape. Squamous metaplasia may ensue with differentiation into typical stratified squamous epithelium. If the rate of cell loss diminishes due to metabolic accommodation to the irritant, the regenerating epithelium will differentiate, but the height of the cells will be increased and there may be increased numbers of serous and goblet cells. The hyperplastic epithelium may also be irregular and folded due to crowding of the cells (Figure 23.17). Regeneration of alveolar epithelium follows a similar pattern. The denuded alveolar basement membrane is first covered by irregular polyhedral cells derived from the proliferating alveolar Type II cells, and the alveolar epithelium becomes simple cuboidal in appearance (Figures 23.18 and 23.19). These cells differentiate and become alveolar Type I cells as the injury diminishes. Prolonged low-level injury may result in metaplasia of the alveolar epithelium, which is characterized by replacement of Type I cells with ciliated cells and Club cells (Figure 23.20). Type II cell hyperplasia is a common response to inhalation of pulmonary toxicants (Miller and Hook, 1990; Schwartz, 1986). With inhaled aerosols or

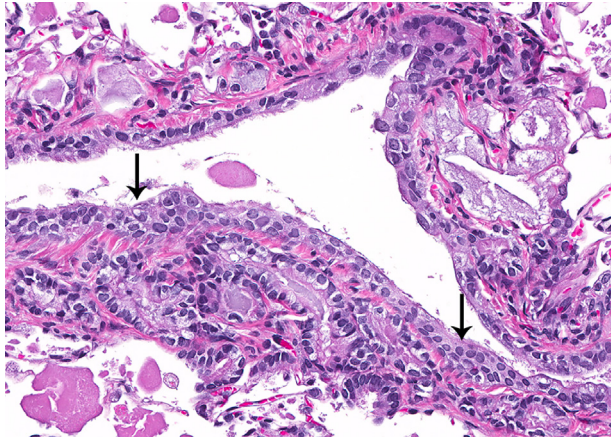


**FIGURE 23.17** Hyperplasia of the bronchiolar epithelium. Note crowding of the epithelium (arrows).

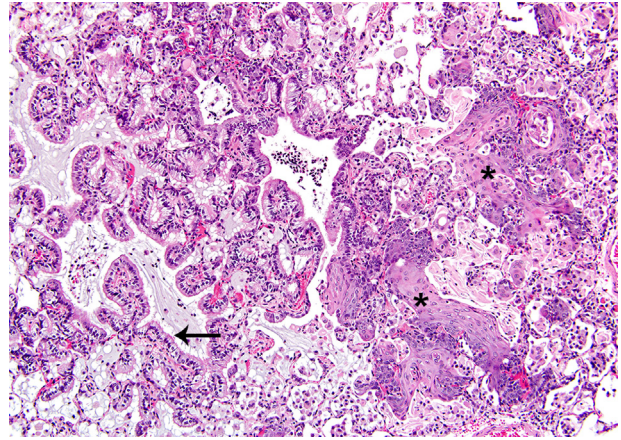


**FIGURE 23.20** Replacement of the alveolar epithelium with ciliated hyperplastic cells (arrow). Note also that the alveolar epithelium is replaced by irregular areas of squamous epithelium (asterisks), a common finding in cases of ongoing prolonged damage.

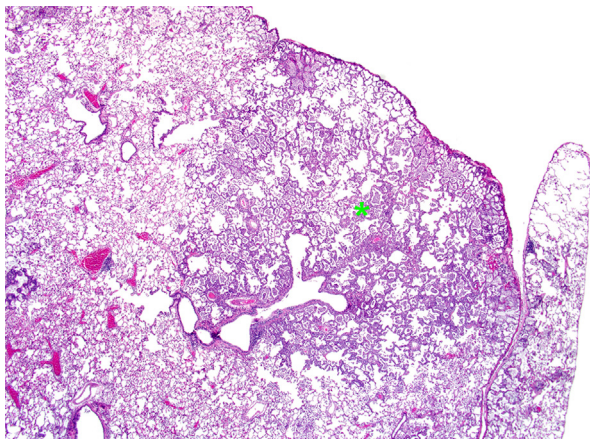


**FIGURE 23.18** Alveolar hyperplasia of the Type II alveolar epithelium characterized by an increase in Type II epithelial cells (asterisk). The underlying alveolar architecture is preserved.

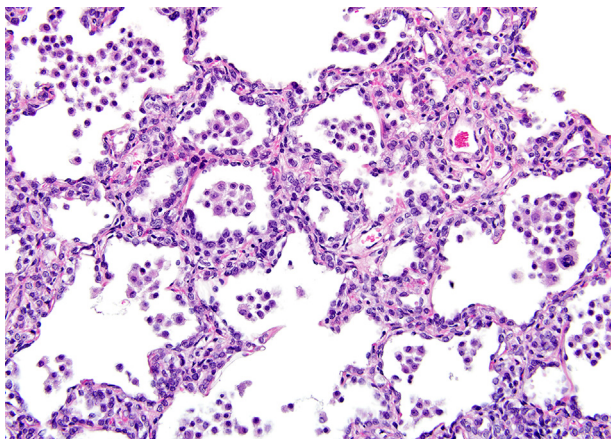


**FIGURE 23.19** Higher magnification of Fig. 23.18. Cuboidal Type II epithelial cells line the alveolar septa. Note increased numbers of macrophages (alveolar histiocytosis) within the alveoli.

particulate matter, the centriacinar region of the lung is most commonly affected. Regenerative hyperplasia of the bronchial or alveolar epithelium is usually accompanied by some degree of inflammation and, if the injury is severe, fibrosis.

## 6.2. Primary Hyperplasia of the Alveolar Epithelium

Focal alveolar epithelial hyperplasia and alveolar/bronchiolar adenoma and carcinoma comprise a morphological continuum. An important feature in distinguishing hyperplasia from adenoma is that the underlying alveolar architecture is maintained in foci of hyperplasia. It is uncertain at what rate focal hyperplasia regresses or progresses to neoplasia, but as long as normal alveolar architecture is retained, a diagnosis of hyperplasia rather than adenoma is warranted. Hyperplasia of the alveolar epithelium is characterized by a focal increase in Type II cells lining the interalveolar septa. The Type II cells may be contiguous, and the alveolar epithelium will be simple cuboidal in appearance (Figures 23.21 and 23.22). The cells may have prominent cytoplasmic vacuoles, but there is no cellular atypia and mitotic figures are not common. The interstitium of affected interalveolar septa is more prominent when the hyperplasia is severe, and there may be an increased number of alveolar macrophages, which contributes to the overall appearance of increased cellularity, but other evidence of inflammation is absent. The boundary of the lesion is usually not sharply demarcated and compression of the adjacent parenchyma is not seen. At the margin of the lesion, proliferating Type II cells extend into adjacent alveoli.

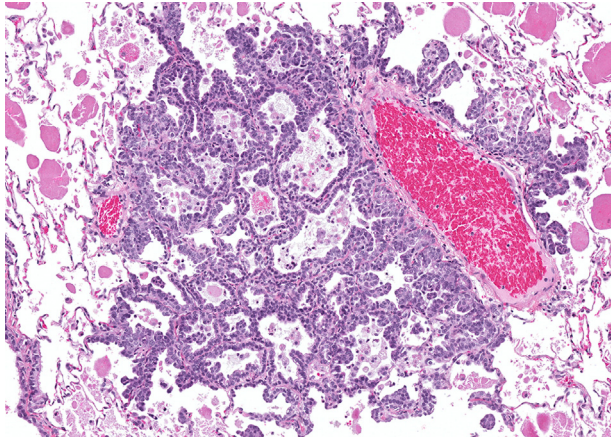


**FIGURE 23.21** Focal alveolar epithelial hyperplasia. The alveolar architecture is essentially maintained, however, there is early distortion.

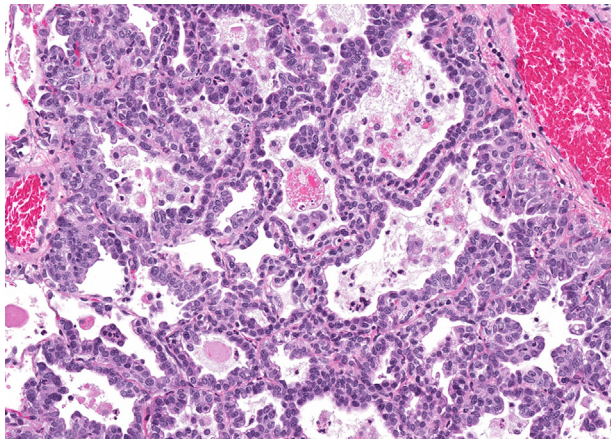


**FIGURE 23.22** Higher magnification of Fig. 23.21. The alveoli are lined by round to cuboidal hyperplastic cells and there is focal piling up and distortion of the hyperplastic epithelium. Note increased numbers of macrophages within the alveoli.

### 6.3. Bronchial Hyperplasia

Hyperplasia of the bronchial epithelium may occur as a regenerative response secondary to injury or as part of the morphological continuum in response to a carcinogen causing bronchial neoplasms. Inflammation associated with focal hyperplasia suggests that the hyperplasia is secondary, whereas hyperplasia occurring in the absence of evidence of tissue injury may be preneoplastic. This lesion is characterized by increased layers of surface respiratory epithelial cells, usually lacking cilia. The proliferating epithelium may project into the airway lumen and may be papillary with small fronds of epithelium supported by a scant connective tissue core (Figure 23.23). Mild nuclear atypia and pleomorphism may be present.

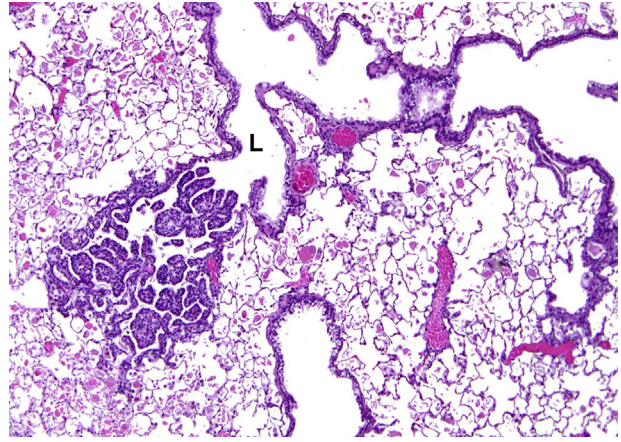


**FIGURE 23.23** Hyperplasia of the bronchiolar epithelium. The hyperplastic cells form papillary projections into the lumen (L).

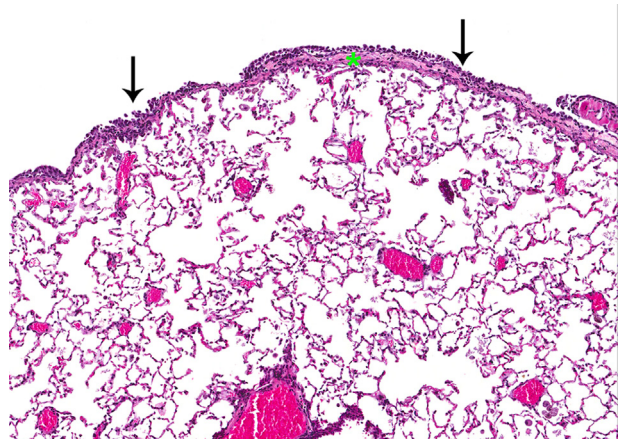


**FIGURE 23.24** Mesothelial cell hyperplasia characterized by hyperplasia and hypertrophy of the mesothelial cells lining the pleura (arrows). Also note the subpleural fibrosis (asterisk).

### 6.4. Mesothelial Hyperplasia

Pleural mesothelial hyperplasia is typically a secondary change associated with a variety of lung diseases including infection, inflammation, thoracic effusions, and pulmonary neoplasms. The lesion consists of focal to multifocal and sometimes diffuse hyperplasia and hypertrophy of mesothelial cells (Figure 23.24). Mesothelial hyperplasia is often accompanied by pleural fibrosis (Figure 23.24) in cases of subpleural inflammation and especially when inflammation is chronic active, and may occur as micropapillary fronds of mature connective tissue covered by a single layer of flattened to cuboidal mesothelial cells (Figure 23.25). Mesothelial hyperplasia is most commonly observed in inhalation studies with instilled or inhaled particulates and is most severe in the parietal pleura lining the diaphragmatic surface of the lung (Everitt et al., 1994, 1997).

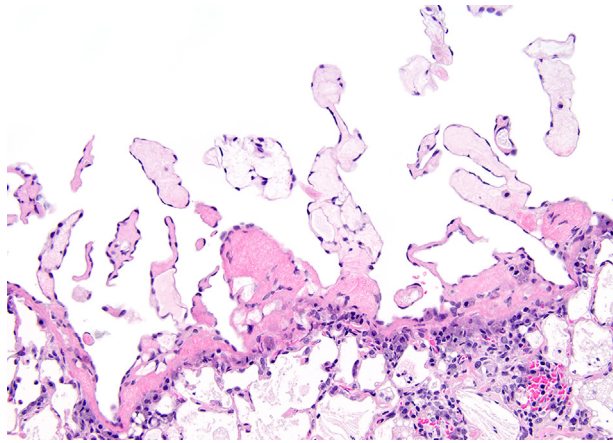


**FIGURE 23.25** Mesothelial hyperplasia occurs as micropapillary fronds of connective tissue lined by a single layer of flat to low cuboidal mesothelial cells. Note pleural fibrosis.

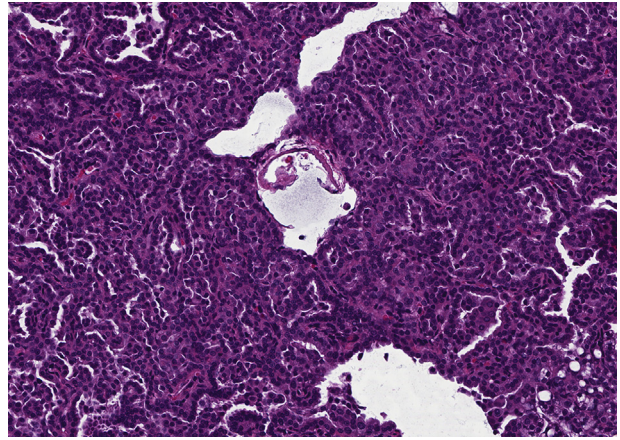


**FIGURE 23.27** Higher magnification of Fig. 23.26. The alveolar/bronchiolar adenoma has a papillary pattern.

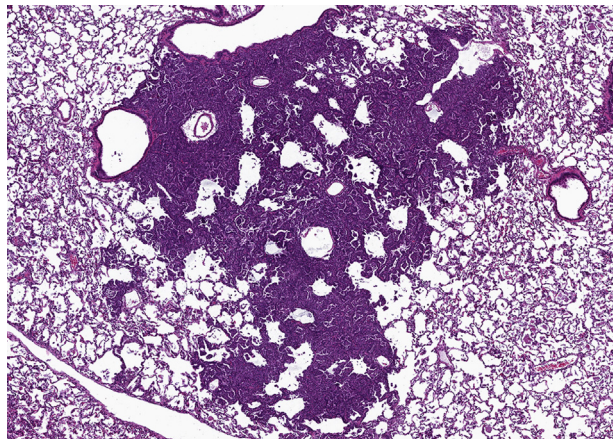


**FIGURE 23.26** Alveolar/bronchiolar adenoma. The alveolar architecture is largely effaced but is still visible in some areas.

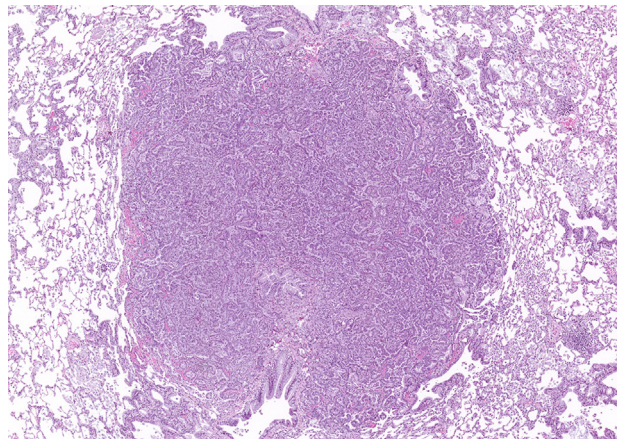


**FIGURE 23.28** Alveolar/bronchiolar adenoma. The alveolar architecture is completely effaced.

### 6.5. Alveolar/Bronchiolar Adenoma and Carcinoma

Grossly, alveolar/bronchiolar adenomas often appear as slightly raised, discrete white to pale yellow, 1–4 mm nodular masses on the surface of the lung. Histologically, adenomas are well-demarcated masses that may cause compression of the adjacent parenchyma and are frequently located at the periphery of the lung (Figures 23.26–23.29). In contrast to hyperplasia, there is distortion of the underlying alveolar architecture. The epithelium may be arranged in three histologic patterns: glandular, papillary, or mixed patterns. The alveolar spaces are obliterated to varying extents, and some neoplasms may appear solid. The epithelium is cuboidal to columnar and overlies a delicate fibrovascular stroma. The neoplastic epithelial cells are relatively uniform with

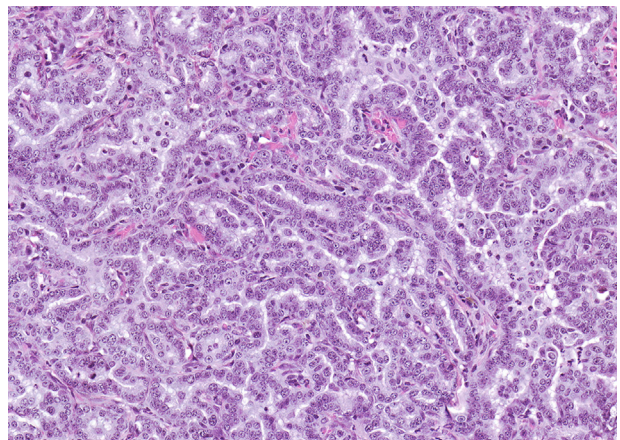


**FIGURE 23.29** Higher magnification of Fig 23.28. Note the distinct papillary growth pattern.

round or oval nuclei and moderately abundant cytoplasm, and some may have apical cytoplasmic vacuoles which probably represent lamellar bodies or lipid droplets (Reznik-Schuller and Reznik, 1982; Ohshima et al., 1985). Neoplastic cells that are columnar tend to have nuclei that are more basal in location and cytoplasm that is more basophilic than that of cuboidal cells. Small, focal areas of mild cellular atypia or pleomorphism may be present—mitotic figures are rare or absent.

Alveolar/bronchiolar carcinomas are often poorly circumscribed (Figures 23.30 and 23.31). However, rapidly growing neoplasms may cause compression of the surrounding parenchyma and appear moderately well demarcated (Figures 23.32 and 23.33). The carcinomas may invade airways (Figures 23.34 and 23.35), pleura, or vessels and metastasize to regional lymph nodes, liver,

kidney, heart, or other organs. Hallmarks of alveolar/bronchiolar carcinomas are their heterogeneous growth patterns and cellular pleomorphism (Figures 23.36 and 23.37). Morphologic growth patterns vary from glandular, papillary, solid, to a mixture of these patterns. Well-differentiated carcinomas with a papillary pattern are difficult to distinguish from adenomas. Stratification of the neoplastic epithelium, solid areas of growth, cellular pleomorphism, and atypia or anaplastic cells associated with a scirrhous reaction and local invasion are indications of malignancy (Figures 23.34–23.37). Alveolar or glandular patterns of growth are usually observed only when there is a prominent connective tissue component or scirrhous reaction. Scirrhous reactions are not commonly seen in spontaneous alveolar/bronchiolar carcinomas, but occur in some carcinomas induced by exposure to particulate che-

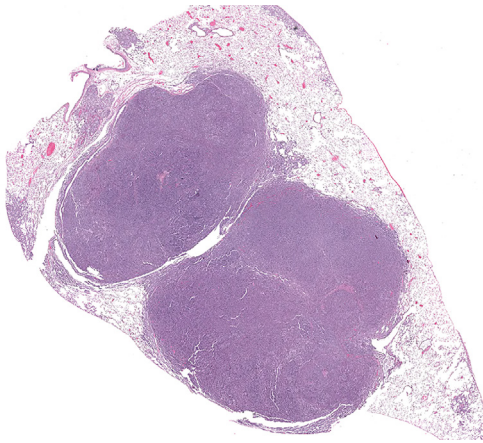


**FIGURE 23.30** Alveolar/bronchiolar carcinoma that is highly invasive and expansive and has largely effaced the lung parenchyma.

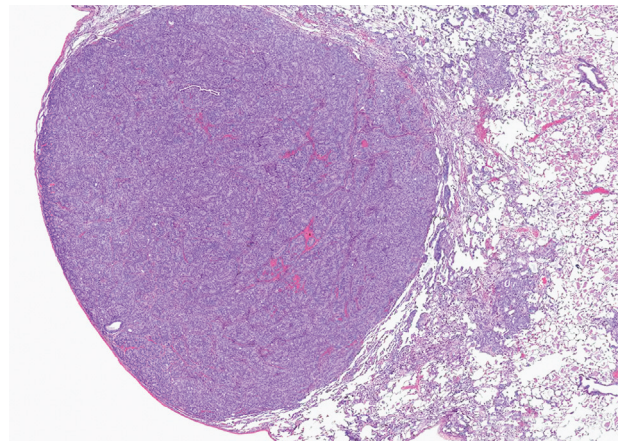


**FIGURE 23.32** Alveolar/bronchiolar carcinoma showing compression of the immediately adjacent lung parenchyma.

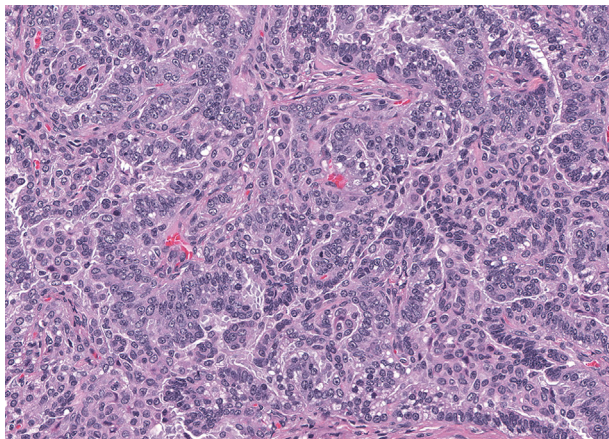


**FIGURE 23.31** Higher magnification of Fig. 23.30. Note the distinct papillary pattern characterized by well- to poorly-defined papillary structures lined by pleomorphic neoplastic cells. In some areas, the papillary structures are supported by irregular strands of fibrous stroma.

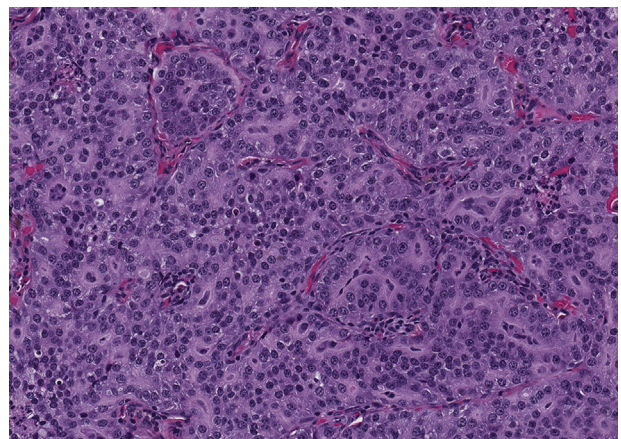


**FIGURE 23.33** Higher magnification of Fig. 23.32. Note glandular growth pattern and solid sheets of cells. Gland-like structures are separated by thin fibrovascular stroma.

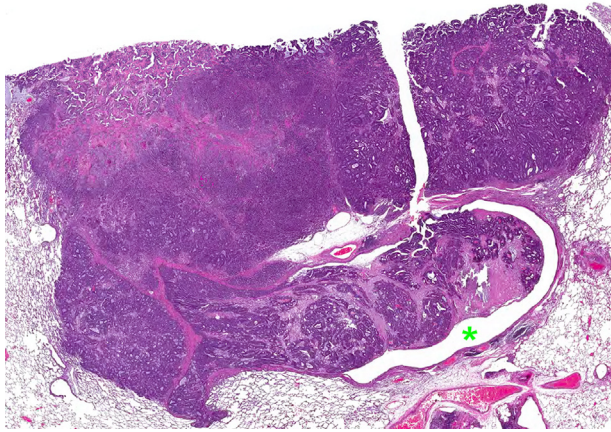


**FIGURE 23.34** Highly invasive alveolar/bronchiolar carcinoma showing invasion into the airway (asterisk).

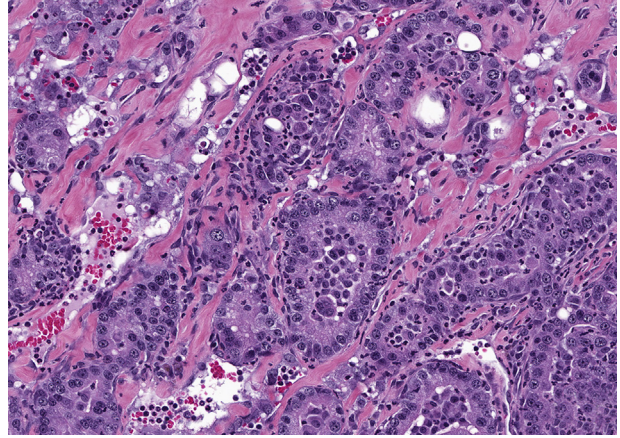


**FIGURE 23.37** Higher magnification of Fig. 23.36. Note heterogeneous growth and anaplastic, pleomorphic cells interspersed with irregular bands of fibrous tissue.

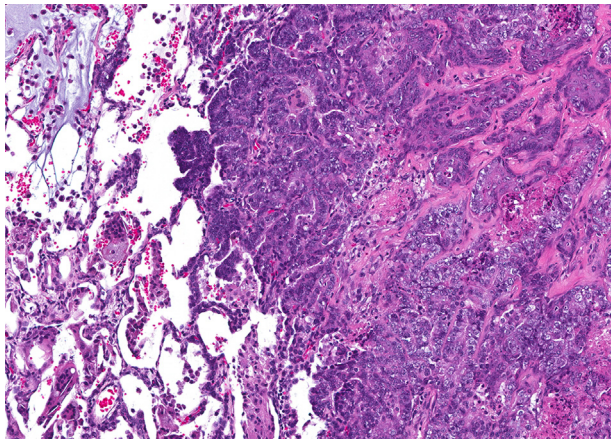


**FIGURE 23.35** Higher magnification of Fig. 23.34. Note poorly defined glandular and papillary pattern and the scirrhous component.

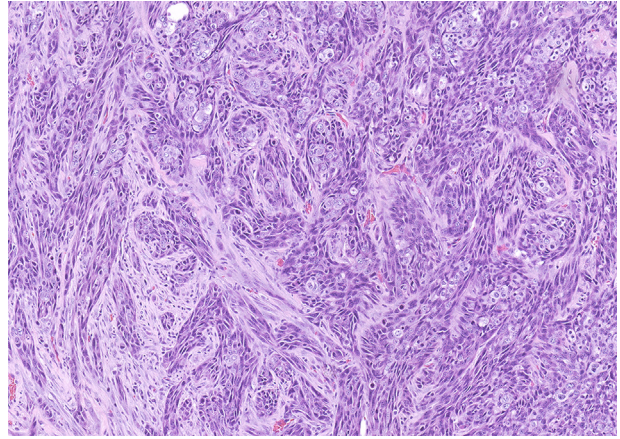


**FIGURE 23.38** Alveolar/bronchiolar carcinoma with anaplastic spindle cell component.

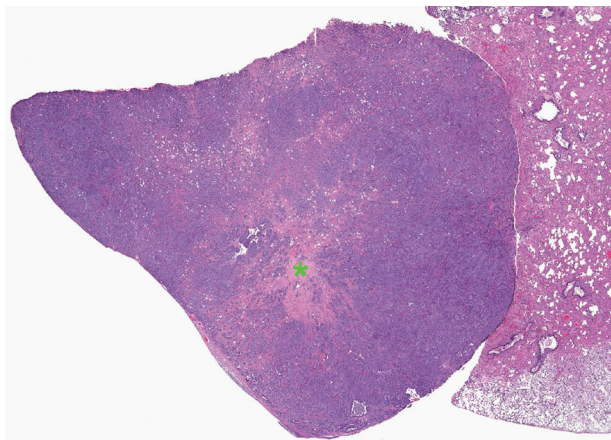


**FIGURE 23.36** Alveolar/bronchiolar carcinoma with a heterogeneous growth pattern and a scirrhous component (asterisk).

micals such as asbestos, silica, gallium arsenide, cobalt sulfate heptahydrate, cobalt metal, and other particulate chemicals. In some small neoplasms, the scirrhous reaction may be so pronounced that the neoplasm appears to arise within an area of fibrosis. Neoplastic cells within a carcinoma may be pleomorphic, and particularly anaplastic cells may be spindle shaped (Figure 23.38). Squamous differentiation is observed in some carcinomas and may be quite prominent (Figure 23.39). However, the diagnosis of squamous cell carcinoma is restricted to neoplasms that consist predominantly of squamous cells. Otherwise, neoplasms with squamous differentiation are classified as alveolar/bronchiolar carcinomas on the assumption that they are more anaplastic variants of alveolar/bronchiolar carcinomas. Neoplastic cells may also differentiate into a mucinous cell type; however, such differentiation is rare. Metastases from spontaneous alveolar/bronchiolar' carcinomas are not commonly observed but may be more

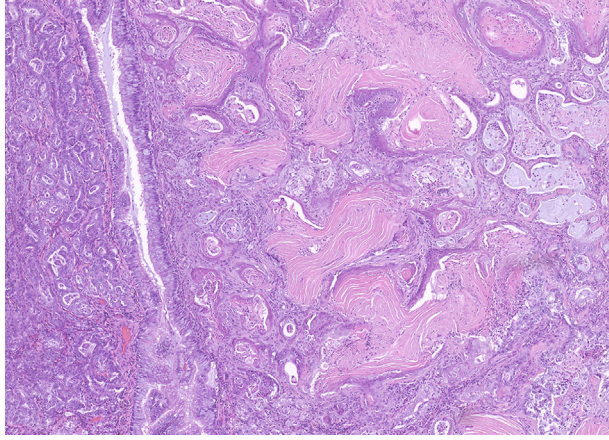


**FIGURE 23.39** Alveolar/bronchiolar carcinoma with papillary and tubular pattern of growth on the left and squamous differentiation on the right.

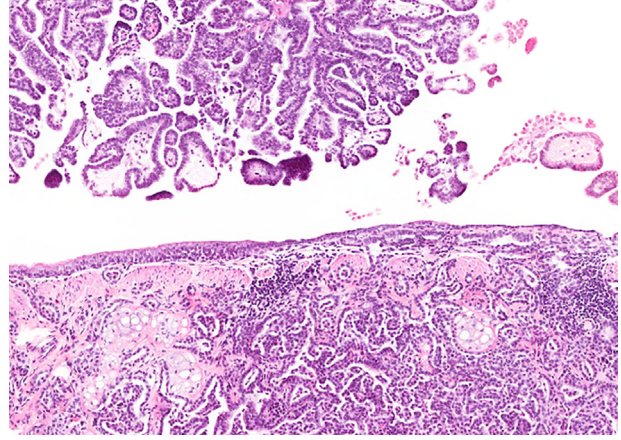


**FIGURE 23.41** Higher magnification of Fig. 23.40.

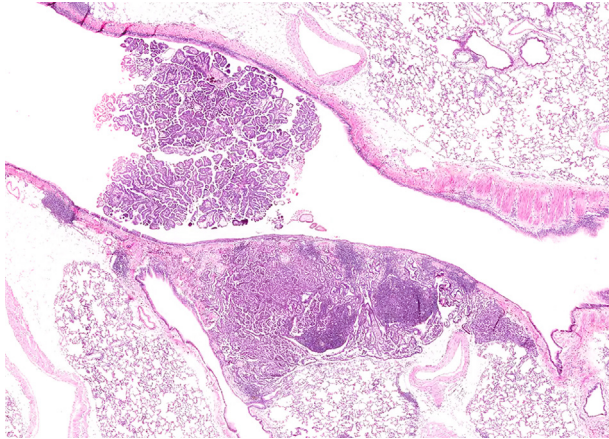


**FIGURE 23.40** Bronchial carcinoma. Note exophytic papillary growth of the neoplastic epithelial cells in the lumen of the bronchus, and invasion into the peribronchial submucosal tissue.

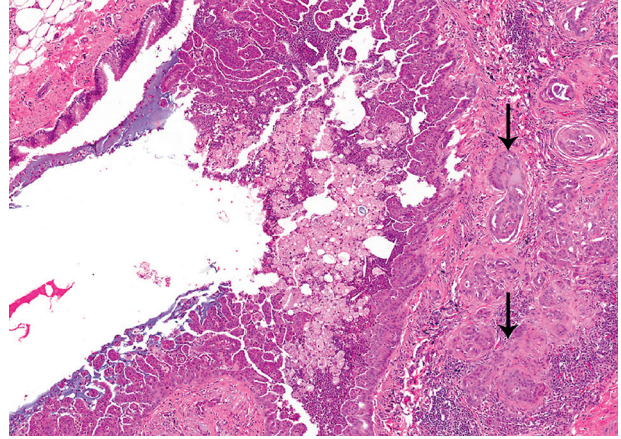


**FIGURE 23.42** Bronchial carcinoma. The neoplastic epithelium (arrows) has invaded the wall of the bronchus.

frequent with induced carcinomas. The metastatic lesions exhibit a papillary or glandular pattern of growth.

## 6.6. Bronchial Adenoma and Carcinoma

The term bronchial adenoma or carcinoma is reserved for neoplasms that clearly arise in the airways. In contrast to the human, where pulmonary neoplasms frequently arise in the large airways, bronchial neoplasms are extremely rare in the F344 rat but can be induced by exposure to carcinogens. The majority of these neoplasms are exophytic papillary or polyp-like masses that protrude into the airway lumen, but endophytic adenomas occurring mainly within the lamina propria may also occur. Large neoplasms may obliterate the airway, making the origin difficult to discern. Adenomas generally have a uniform growth pattern that may be papillary, glandular, or mixed. The neoplastic

epithelium consists of uniform cuboidal to columnar cells with little or no cellular pleomorphism or atypia.

Bronchial carcinomas may have an exophytic papillary or glandular growth pattern and project into the airway lumen or invade the bronchial wall (Figures 23.40–23.42). Carcinomas are distinguished from adenomas on the basis of cytological features indicative of anaplasia or evidence of invasion. The overlying bronchial epithelium may appear relatively normal and the neoplasm is mainly in the lamina propria of the airway. Since submucosal glands do not occur at this level of the airways, this neoplasm most likely originated from the respiratory epithelium of the bronchus.

## 6.7. Squamous Cell Carcinoma

Spontaneously occurring squamous cell carcinomas of the lung are rare in the F344 rat, although inhalation or

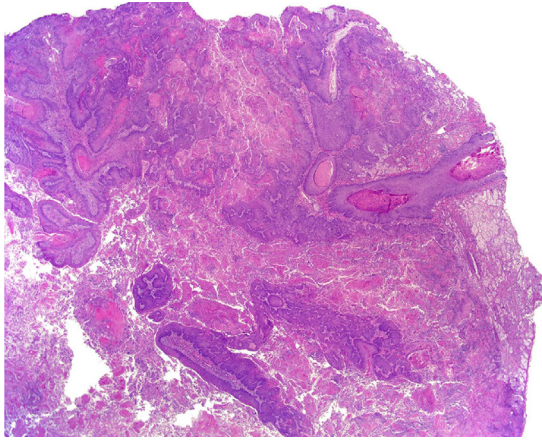


**FIGURE 23.43** Squamous cell carcinoma of the lung.

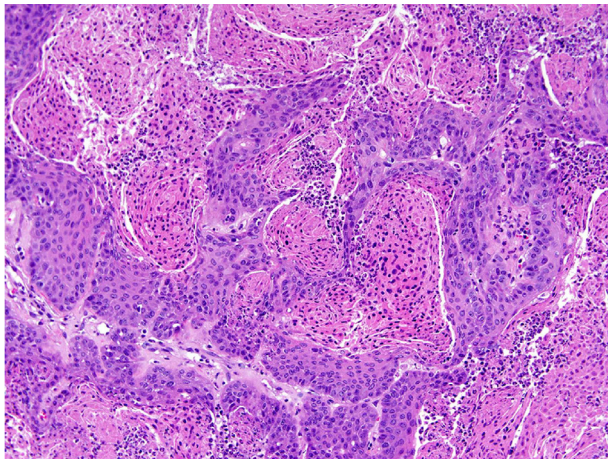


**FIGURE 23.44** Higher magnification of Fig. 23.43. Note irregular bands of neoplastic squamous epithelium interspersed with necrotic epithelial cells.

instillation of chemical agents may induce this neoplasm (Dixon et al., 2008). The site of origin of the pulmonary squamous cell carcinomas in the F344 rat is uncertain. Although this neoplasm may arise from areas of squamous metaplasia in the bronchi, bronchioles, or alveoli, it may also arise from keratinizing cysts originating in the alveoli. Squamous cell carcinomas efface the normal architecture of the lung and often produce abundant keratin (Figures 23.43 and 23.44), however there is variability in keratin production between neoplasms. They are highly invasive extending into the contiguous alveolar parenchyma, may induce a marked necrosis and/or scirrhous response, and may metastasize. The neoplastic cells form irregular cell clusters, nests, or islands of squamous epithelial cells with or without central keratinization (keratin pearls). The neoplastic squamous cells may be markedly pleomorphic, including the formation of large atypical giant cells. Poorly keratinized or nonkeratinized variants

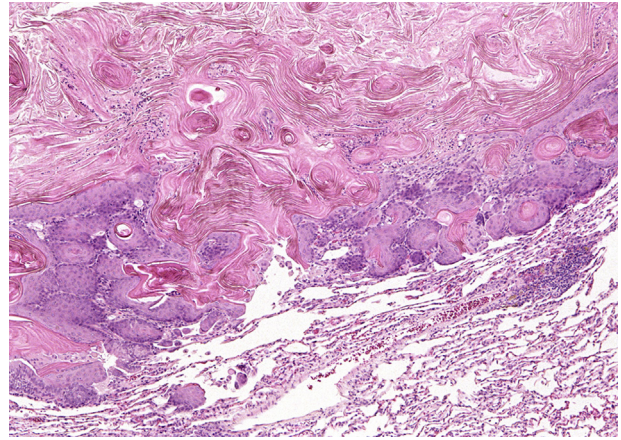


**FIGURE 23.45** Cystic keratinizing epithelioma in the lung. Note central, cystic cavity that contains laminated keratin and keratin whorls (pearls), surrounded by a complex wall of squamous epithelium.

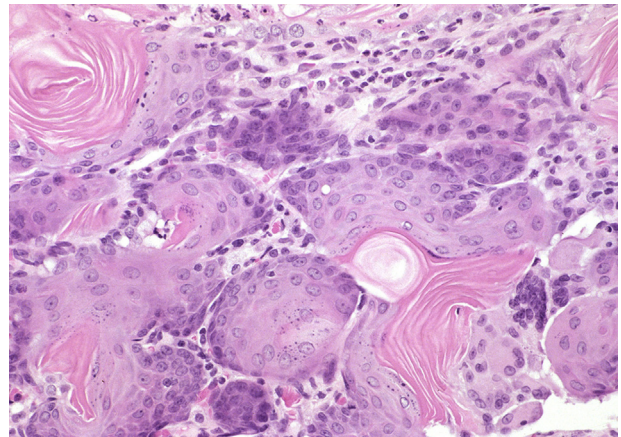


**FIGURE 23.46** Higher magnification of Fig. 23.45. The wall is composed of well-differentiated squamous epithelium.

of squamous cell carcinomas have distinct intercellular bridges.

Squamous cell carcinomas must be distinguished from CKE, which have been reported following chronic inhalation exposure to high concentrations of inert particles. Keratinizing cysts are discussed further under miscellaneous lesions. Squamous cell carcinoma that have a large central mass of keratin and necrotic debris are thought to arise from the walls of benign keratinizing cysts and must be distinguished from CKE. In rats, large squamous cell carcinomas may frequently metastasize to or invade the mediastinum and the mediastinal and bronchial lymph nodes.

### 6.8. Cystic Keratinizing Epithelioma

In rats, spontaneous CKE are rare. They most often observed after inhalation exposure to diverse particulates

and other chemicals (Dixon and Maronpot, 1991; Boorman et al., 1996; Walker et al., 2007; Rittinghausen and Kaspareit, 1998; Rittinghausen et al., 1997; Mohr et al., 2006) and must be distinguished from squamous cell carcinomas. These neoplasms are considered to arise from areas of squamous metaplasia in the alveolar epithelium and Club cells, or focal squamous cysts. CKE are discretely irregular, small to expansive cystic lesions that are sharply demarcated from the surrounding alveolar parenchyma (Figures 23.45 and 23.46). Compression of the adjacent lung parenchyma is usually not observed except in association with larger neoplasms, as growth seems to occur by extension along contiguous alveolar septae from the periphery of the wall. The neoplasm consists of a central, cystic cavity filled with laminated keratin and keratin whorls (pearls), surrounded by a complex wall of squamous epithelium that shows no atypia, dysplasia (abnormal or disorderly differentiation), or invasive growth. The squamous wall varies in thickness, consisting of three to several layers of mature, well-differentiated, squamous epithelium and irregular nests and islands of squamous epithelium that extend along adjacent alveoli resulting in an irregular border. In toxicology/carcinogenicity studies in which increased incidences of CKE occur, the extrapolation and relevance of this finding to human health is incompletely understood since CKE do not occur in the human lung. Therefore, when CKE occurs as a treatment related change in a carcinogenicity study, its relevance to human health should be decided on case-by-case basis, considering other changes and available data (Boorman et al., 1996; Walker et al., 2007).

### 6.9. Sarcoma

Some alveolar/bronchiolar carcinomas in the rat contain a prominent component of spindle-shaped cells. When there is good morphologic evidence of an epithelial component in a tumor with sarcomatous areas, the most appropriate diagnosis is carcinoma. However, some pulmonary neoplasms appear to be entirely mesenchymal with no glandular or epithelial areas. These are considered to be mesenchymal in origin and should be classified accordingly. They occur rarely in the F344 rat. Fibrosarcoma (Figure 23.47), leiomyoma, and leiomyosarcoma have been observed and are most often metastatic. The morphological features of these neoplasms are similar to those found in other organs and are not described in detail here. Occasionally, metaplastic foci of cartilage or bone are found within a fibrosarcoma. Well-differentiated neoplasms of smooth muscle origin may arise in the wall of bronchi or vessels. Anaplastic sarcomas of uncertain histogenesis are also occasionally observed.

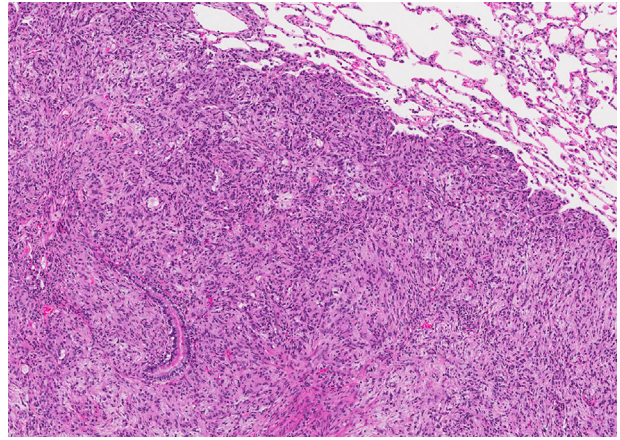


**FIGURE 23.47** Fibrosarcoma of the lung composed haphazardly arranged spindle cells.

### 6.10. Malignant Mesothelioma

Mesotheliomas in the thoracic cavity arise from the mesothelial cells lining the pleura. Primary spontaneous pleural mesotheliomas are rare in rats. They have been induced by exposure to various fibers and chemicals (Greaves et al., 2013; Kane, 2006; Doi et al., 2010; Wagner, 1962; Stanton and Wrench, 1972). Grossly, pleural mesotheliomas may be focal or diffuse along the pleura, and grow by expansion rather than infiltration. In rats, all mesotheliomas are considered malignant. Histologically, pleural mesotheliomas may be classified as epithelial, mesenchymal, or a mixture of both (Stanton and Wrench, 1972; Wagner and Berry, 1969; Davis, 1979). Epithelial mesotheliomas are the most common histologic type and may be classified as papillary, tubular, tubulopapillary, or solid. The papillary type is most prevalent and are usually exophytic consisting of single or multiple, irregularly branching, frond-like proliferations of well-vascularized collagenous to fibrous connective tissue stroma lined by a single to several layers of uniformly small, low cuboidal to polyhedral mesothelial cells (Figures 23.48 and 23.49). The tubular type consists of large atypical pleomorphic cells that form glandular-like structures. The solid type can be quite extensive, florid proliferations composed of abundant prominent stroma with extensive areas of pleomorphic mesothelial cells occurring as clusters, tubular structures, and solid sheets on the surface and within the masses. The mesenchymal variant resembles fibrosarcomas and consists of interlacing bundles of spindle shaped cells that resemble fibroblasts. The mixed variant has both epithelial and mesenchymal components occurring together in varying proportions.

Most pleural mesotheliomas do not present a diagnostic challenge. However, it is may be difficult to distinguish those with a significant mesenchymal component from pleural metastases, thoracic sarcomas, reactive

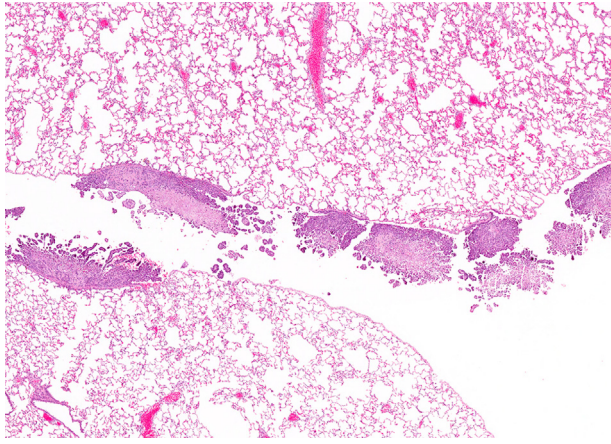


**FIGURE 23.48** Malignant mesothelioma of the lung characterized by multifocal papillary neoplastic mesothelial cells on the surface of the pleura.

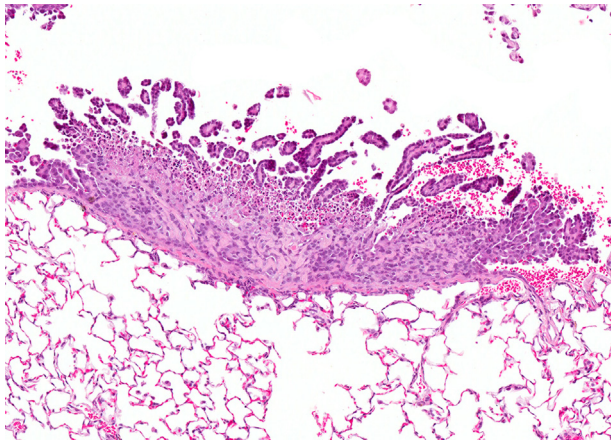


**FIGURE 23.49** Higher magnification of Fig. 23.48. Note characteristic multiple, frond-like proliferations lined by a single layer of uniformly small, low cuboidal to polyhedral mesothelial cells associated with fibrous thickening of the pleura.

pleural lesions, and some primary lung neoplasms particularly those with a sarcomatous pattern. In such cases, immunohistochemical staining may be a useful aid for differential diagnosis. Proper controls should be included during immunohistochemistry as many of the antibodies used for diagnosing mesotheliomas in humans are not optimized for rat tissues. Ultrastructurally, the presence of neoplastic cells that have numerous microvilli and intercellular junctions may also be suggestive of malignant mesothelioma (Davis, 1979).

### 6.11. Mediastinal Neoplasms

Primary mediastinal neoplasms are uncommon in rats. Mediastinal neoplasms may arise from mediastinal tissues, but more commonly are metastases from primary malignant neoplasms that develop in almost any tissue or organ. Benign thymomas typically occur in the anterior

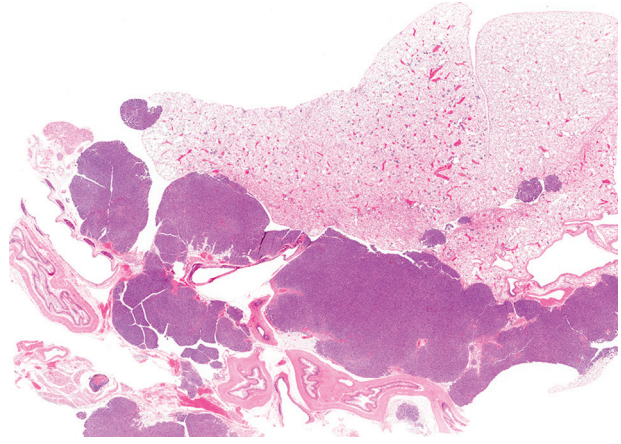


**FIGURE 23.50** Alveolar/bronchiolar carcinoma invading the mediastinum of the lung.

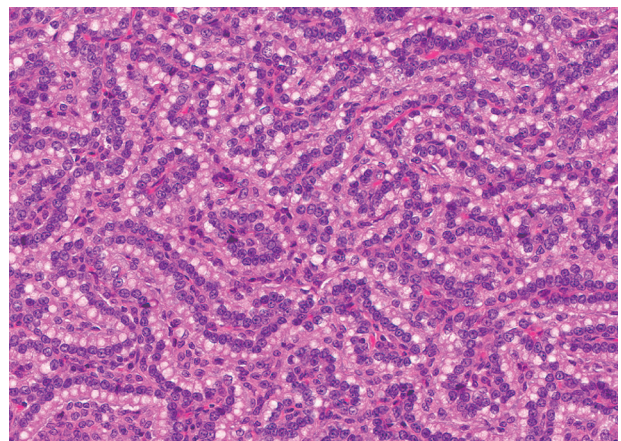


**FIGURE 23.51** Higher magnification of Fig. 23.50. Note that the neoplasm consists of distinctly papillary structures composed a delicate vascularized stroma lined uniformly cuboidal neoplastic cells with apical cytoplasmic vacuoles reminiscent of alveolar Type II cells.

mediastinum and malignant thymomas may invade the mediastinum. Thoracic mesotheliomas and alveolar/bronchiolar carcinomas (Figures 23.50 and 23.51) have the potential to metastasize to the mediastinum. Rare neoplasms that occurred entirely or largely free in the mediastinum have been reported in rats from studies conducted by the National Toxicology Program. These neoplasms had an alveolar/bronchiolar histologic pattern and were immunopositive for Club (Clara) cell secretory protein suggesting that they were probably of alveolar/bronchiolar origin despite the predominantly mediastinal location (Howroyd et al., 2009).

### 6.12. Metastatic Neoplasms

The lung is the most common site of metastasis of neoplasms in rats due to its extensive supply of small caliber

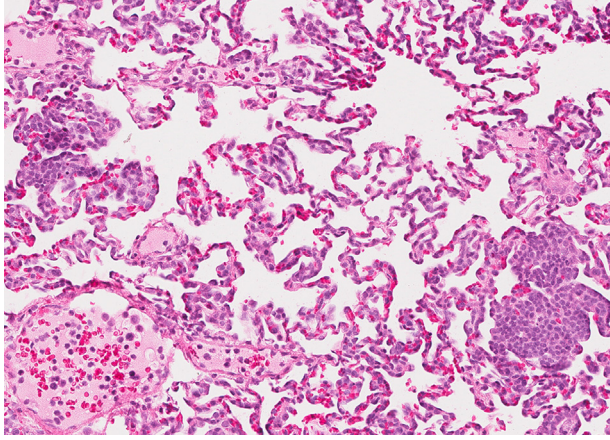


**FIGURE 23.52** Mononuclear cell leukemia in the rat lung. Note lymphocytes within blood vessels and capillaries.

blood vessels and lymphatics. Metastatic neoplasms are mostly epithelial and tend to be multiple. Common primary sites of origin of neoplasms metastatic to the lungs of rats include the skin, bone, mammary gland, Zymbal's and harderian gland, and liver. Metastatic neoplastic cell emboli are often observed in pulmonary blood vessels and lymphatics. Intrapulmonary metastasis is often seen with chemically induced alveolar/bronchiolar carcinomas and occurs via the lymphatics. Extrapulmonary metastases of alveolar/bronchiolar carcinoma have been identified in the mediastinum. Systemic hematopoietic/lymphoid neoplasms such as mononuclear cell leukemia and histiocytic sarcoma are common in the lungs of aged rats. These neoplasms arise within the spleen and other lymphoid organs, and tend to be diffuse within the lung and may resemble inflammatory lesions. The circulating neoplastic cells are observed in the pulmonary capillaries and cause increased cellularity (Figure 23.52). In addition to the increased cellularity, hemorrhage and thrombosis may be associated with the infiltrating cells.

## 7. MISCELLANEOUS LESIONS

### 7.1. Gavage-Related Lesions

Chemicals may be administered to experimental animals by oral gavage because they are insoluble in water or because of poor palatability. Corn oil is the vehicle for lipid-soluble chemicals commonly used in studies sponsored by the National Toxicology Program. With unexpected early death in a gavage study, it is necessary to determine whether the death is related to the chemical or is the result of improper gavage technique. Gavage-related deaths are usually due to perforation of the esophagus and deposition of the material in the pleural cavity or asphyxiation as a result of deposition of the material in the lungs. Toxic agents given by gavage may make the

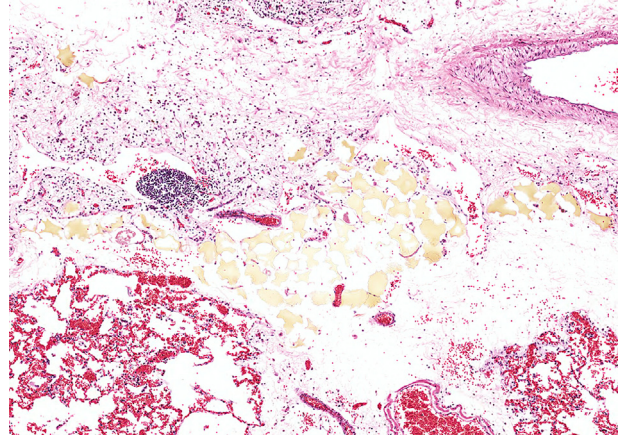


**FIGURE 23.53** Gavage-related lesion in the lung. Note golden yellow gavage vehicle (oil) within the lung associated with chronic inflammation, hemorrhage, and congestion.

rat lethargic following dosing and thus more prone to inhalation of the vehicle from the oropharynx. This may result in a dose-related mortality that further complicates identification of gavage-related deaths in the study.

Perforation of the esophagus and evidence of dosing solution in the pleural cavity or evidence of the chemical or oil vehicle in the lung are definitive, but lack of gross findings does not rule out a gavage-related death. When the gavage material is deposited in the lungs, the histological findings often are not striking. This is particularly true in control animals given the vehicle only. Pronounced congestion of the pulmonary capillaries and droplets of oil in the lung are helpful findings (Figure 23.53). Solvents used in histological processing will dissolve much of the oil vehicle, so none or little will be seen in the tissue section. Ancillary information such as time of death relative to that of gavage and lack of other pathological changes that might explain the cause of death should be taken into consideration. Inhalation of foreign material may not be immediately fatal, and the material may cause a foreign body reaction with the development of granulomatous, inflammation. When this occurs in the airway, the epithelium may cover the reaction, creating an epithelium-covered inflammatory nodule.

### 7.2. Hair Embolism

Hair emboli are occasionally found in the lung following intravenous injection. The keratin of the hair is easily seen with polarized light. In most cases, the hair fragment is surrounded by an inflammatory infiltrate. Hair fragments initially induce an acute inflammatory reaction with an accumulation of granulocytes followed by the formation of microgranulomas. Some hair fragments remain for many weeks before the lesions are resolved (Kast, 1966).

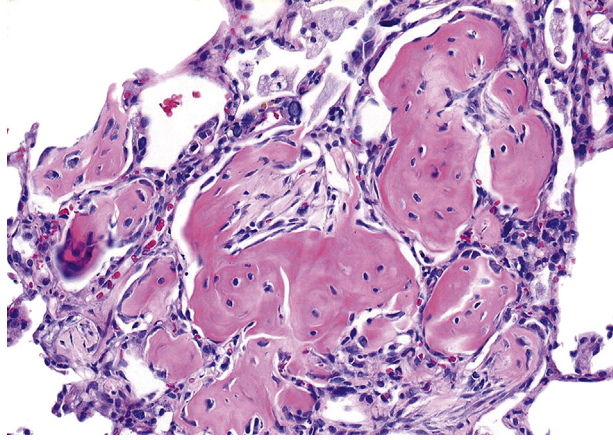


**FIGURE 23.54** Osseous metaplasia in the lung consisting of irregular clusters of woven bone.

### 7.3. Cartilaginous Metaplasia

Small foci of mature cartilage are occasionally observed in the rat lung. The biological behavior of this incidental lesion is unknown. In humans, a similar lesion has been termed cartilaginous hamartoma, but is now considered a benign neoplasm. When this lesion is found in a rat, it is important to consider metastatic chondrosarcoma. A single focal lesion lacking cellular atypia and the absence of a primary chondrosarcoma suggest cartilaginous metaplasia rather than neoplasia.

### 7.4. Osseous Metaplasia

Small spicules of bone are occasionally found in the lungs of older rats. Osseous metaplasia is characterized by foci of immature woven bone or dense lamellar bone (Figure 23.54). Care must be taken to rule out metastatic osteosarcoma.

### 7.5. Goblet Cell Metaplasia

Goblet cells are not normally found in distal small airways and bronchioles of rats. Goblet cell metaplasia can occur in these distal airways as a response to chronic irritation following exposure to chemicals, or due to infectious disease (Kittel, 1966). This lesion may also arise from blockage of an airway, preventing clearance of material from the affected region of the lung. Hypertrophied goblet cells are increased in number in the affected bronchioles and the distal airways and alveoli may be filled with mucus.

## 8. TOXICOLOGIC LESIONS

Chemicals causing pulmonary toxicity include inhaled particles, gases, and liquid aerosols that exert their effect

directly on the lung parenchyma and agents given systemically that reach the lung via the circulation. The Club cells of the lung contain the cytochrome P-450 monooxygenase system (Plopper, 1983; Boyd, 1984), which is capable of metabolic activation or deactivation of toxicants. The importance of the metabolic capability of Club cells in acute chemical-induced lung injury has been demonstrated experimentally by the preferential damage to Club cells by 4-ipomeanol, 3-methylfuran, and carbon tetrachloride (Doster et al., 1983; Gram, 1989; Haschek et al., 1983; Boyd, 1984).

### 8.1. Toxicity of Particles

The toxicity of inhaled particles is determined to a large extent by the site of deposition in the lung. For very small particles (generally less than 1  $\mu\text{m}$ ) which are deposited primarily by diffusion, particle size is the major factor determining the site of deposition. For larger particles density and shape become more important. Particles that are not spherical in shape are often characterized in terms of equivalent spheres on the basis of equal mass, equal volume, or aerodynamic drag. The aerodynamic diameter is calculated by taking into account the density of the particle and the aerodynamic drag, and it represents the diameter of a unit-density sphere having the same terminal settling velocity as the particle, regardless of its size, shape, and density. The aerodynamic diameter is an appropriate measurement for particles that are deposited by impaction and sedimentation.

Particles are deposited in the lung as a result of interception (important only for fibers such as asbestos), impaction, sedimentation, and diffusion. Particles with an aerodynamic diameter of 5–30  $\mu\text{m}$  are primarily deposited in the nasopharynx and bifurcations of the upper airways by impaction due to the higher air velocity in these regions and the inertia of the larger particles. Particles with an aerodynamic diameter of 1–5  $\mu\text{m}$  are deposited in the bronchial regions by sedimentation. The slower airflow in the bronchi allows time for deposition by gravitational forces. Particles less than 1  $\mu\text{m}$  that have reached the alveoli are deposited primarily by diffusion.

Particles that are deposited on the ciliated epithelium of the airways are cleared from the lung by the mucociliary apparatus, whereas those reaching the alveoli are phagocytized by alveolar macrophages and then cleared by the mucociliary apparatus or removed by lymphatic drainage from the interstitium. The factors influencing the movement of macrophages to the bronchioles or into the interstitium are uncertain.

Inhalation of particles or dusts can result in increased lung weights associated with inflammatory infiltrates. Particulate materials that are reactive and cytotoxic incite an acute inflammatory reaction. The more inert particulate

materials induce primarily an accumulation of alveolar macrophages. Depending on the relative cytotoxicity of the material, there is variable hyperplasia and hypertrophy of Type II cells in the alveolar ducts and alveoli.

The toxicity of relatively inert particles such as talc, plaster of Paris, silica, and titanium dioxide has been evaluated in long-term inhalation studies in rats. There appears to be no truly “inert” particle, since prolonged exposure to particulate materials results in accumulation of alveolar macrophages. When the lung clearance mechanisms are exceeded following inhalation of high concentrations of these materials for long periods, the particles accumulate in the lung with chronic active to chronic inflammation of varying severity. Cholesterol clefts are often found in some of these lesions. Proliferation of ciliated cells and Club cells in the alveolar ducts and proximal alveoli (so called “bronchiolization”), hypertrophy and hyperplasia of Type II cells in the alveoli of the centriacinar region, and squamous metaplasia are observed.

Accumulation of phospholipids in alveoli (alveolar proteinosis or lipoproteinosis) also occurs with exposure to many particulates, particularly silica. Short-term exposure to high concentrations of silica induces a more severe degree of alveolar proteinosis, whereas prolonged exposure to low concentrations induces fibrosis and little alveolar proteinosis. Eventually, fibrosis occurs in the lungs of rats exposed to particles for prolonged periods. The mechanism of fibrosis is still not clear, but may be related to the release of fibrogenic cytokines by inflammatory cells present in the lungs. Some of the inhaled particles enter the interstitium and are phagocytosed by fibroblast-like cells.

Of particular interest are the squamous keratinizing cysts and CKE which have occurred in the lungs of rats exposed to high concentrations of particulate material. These cystic lesions may develop from foci of squamous metaplasia, which also occur in the alveolar regions of rats exposed to these particles. The biological behavior of these lesions is unknown. Although squamous cysts may simply represent a metaplastic response, they may also represent early stages in the development of squamous cell carcinoma or have the potential for progression to squamous cell carcinoma.

Among the particulate materials, those that have been most widely studied are the asbestos fibers. The primary interest in asbestos is due to its ability to cause mesothelioma, pulmonary fibrosis, and primary lung carcinoma in humans. The acute lesions associated with inhalation of asbestos fibers in the rat are infiltrates of alveolar macrophages in the centriacinar region with thickening of the interstitium and hyperplasia of Type II cells. Asbestos fibers cause fibrosis in long-term (two years) inhalation studies in the rat, similar to what occurs in humans. The

degree of pulmonary injury varies with the type of asbestos fiber. Chrysotile asbestos is the most fibrogenic, crocidolite is less active, and amosite is least active. Fiber deposition in the lung is dependent to some extent on fiber length—fibers longer than 11  $\mu\text{m}$  are less likely to be deposited in the lung than those shorter than 11  $\mu\text{m}$ . However, once deposited, the longer fibers are less likely to be cleared from the lung and therefore are more fibrogenic than the shorter fibers. Although fiber length and shape are important determinants of fibrogenicity, the availability of reactive groups on the surface of the asbestos fibers may contribute.

Although fibers such as chrysotile asbestos are rapidly ingested by alveolar macrophages, broken into smaller fragments, and carried from the lung, some of the fibers penetrate the alveolar wall and reach the interstitium. Through incomplete degradation of the fibers and death of the macrophages, small fragments are released into the interstitial tissue and subsequently undergo phagocytosis by fibroblasts. The macrophages may release fibroblast-stimulating factor, and the processes are repeated until a fibrous scar is formed.

The neuroendocrine cells of the airways also proliferate in the bronchioles of rats in response to chronic inhalation of asbestos fibers. In contrast to observations in humans, asbestos bodies (formed by the deposition of proteins and calcium and iron salts on the asbestos fibers) are formed in rats rarely and apparently only when the fibers exceed 10  $\mu\text{m}$  in length.

Inhalation of a variety of gases that contain particulate material also causes accumulation of macrophages (many containing pigment) and lymphocytes in the centriacinar region of the lung with proliferation of Type II cells. Subpleural foci are also found. In addition to the inflammatory cell response, there is moderate fibrosis with prolonged exposure.

## 8.2. Toxicity of Gases

Toxic gases are taken up by the tissues of the respiratory tract at all levels, beginning with the nasopharynx. The uptake of gas is determined by the concentration of the gas in the inspired air and the rate of diffusion. Solubility in water is generally the major characteristic determining the relative toxicity of gases. However, inhaled gases may react chemically with the components of the mucous layer overlying the airway epithelium, thus limiting diffusion or detoxifying the gas. Highly reactive chemicals such as anhydrous acids or strong oxidants can react directly with the lining epithelium of the airways or alveoli and cause necrosis. Less reactive gases such as nickel carbonyl may diffuse through the epithelium without apparent injury and cause necrosis of capillary endothelial cells.

Volatile chemicals that are highly reactive, such as methyl isocyanate (MIC), cause necrosis of the respiratory epithelium of the nose, trachea, bronchi, and bronchioles. Necrosis and ulceration of the epithelium result in accumulation of fibrinous exudate in the airways, infiltration of the fibrin by proliferating fibroblasts, and eventually intraluminal fibrosis. These fibrous lesions become covered by epithelium and may obstruct the air flow in the affected airways. At lower concentrations, there is hyperplasia of the respiratory epithelium with an increased number of goblet cells, which may extend into the terminal bronchioles, where they replace the Club cells.

Inhalation of gases that are less reactive and less irritating than MIC causes lesions primarily in the centriacinar region of the lung; the larger airways generally are not affected as severely. These gases include common urban pollutants such as ozone and nitrogen dioxide. The particular sensitivity of the terminal bronchioles, alveolar ducts, and proximal alveoli may be related to the decreased thickness of the mucous blanket in this area and not to a unique sensitivity of these cells to toxic agents. With mild injury, one of the first changes is focal loss of cilia from the respiratory epithelium and loss of the apical blebs from the Club cells. Higher concentrations lead to concentration-dependent cell necrosis in the terminal bronchioles with compensatory proliferation of Club cells. In the alveoli, the Type I cell is more sensitive to injury than the Type II cell, which may be due to its larger surface area. Compensatory proliferation of Type II cells is seen in most cases of alveolar injury. There is a mild inflammatory reaction with accumulation of alveolar macrophages and an increase in thickness of the blood-air barrier due to collagen deposition in the interstitium with chronic injury. Chronic exposure to nitrogen dioxide has been reported to cause an increase in the number of neuroendocrine cells of the bronchioles.

### 8.3. Toxicity of Chemicals Administered Systemically

Chemicals administered by oral gavage, dosed feed, or dosed water may also cause pulmonary damage. Ingestion of paraquat, a quaternary ammonium bipyridyl herbicide, causes a severe progressive pulmonary fibrosis that can be lethal. The pulmonary toxicity of paraquat resembles that of several other lung toxins, including oxygen, nitrofurantoin, and bleomycin. Following the ingestion of paraquat, there is extensive necrosis of alveolar epithelial cells resulting in completely denuded alveolar basement membranes and severe pulmonary edema. This is followed by proliferation of fibroblasts in and on the alveolar walls with eventual fibrosis. Bleomycin initially causes degeneration and necrosis of capillary endothelial

cells and subsequently alveolar epithelial cells with eventual fibrosis.

Some chemicals affect a specific cell type in the lung—*O,S,S*-Trimethyl phosphorodithioate and 4-ipomeanol cause degranulation and necrosis of Club cells. The selective toxicity of these chemicals to Club cells is due to the mixed-function oxidase system within Club cells and their ability to metabolize certain xenobiotics to more reactive metabolites.  $\alpha$ -Naphthyl thiourea is a toxin that is uniquely toxic for the rat, with primary damage in the endothelium of pulmonary capillaries and venules. Gaps appear in the endothelium and result in pulmonary edema and massive pleural effusions. The mechanism of injury is unknown, and in rats that recover there is no histologic evidence of damage to any lung cells.

Chemicals that have a primary effect on other tissues may induce secondary effects in the lung. It has been shown that experimental bile duct ligation will cause dramatic thickening of alveolar septa and proliferation of Type II cells.

### 8.4. Carcinogenesis

In NTP studies, the lung is not a common site for a carcinogenic response in the F344 rat. In inhalation carcinogenesis studies conducted by the NTP, the lung was positive eight times for male rats and nine times for female rats. The highest incidence of lung neoplasms occurred in rats exposed to tetranitromethane by inhalation. Activated K-ras oncogenes were detected in the neoplasms of male and rats. The cell of origin was not determined in these studies, but they appeared to be typical alveolar/bronchiolar neoplasms.

With genotoxic chemicals or chemicals that cause neoplasms at multiple sites, the induction of pulmonary neoplasms is not entirely unexpected. However, studies have demonstrated that prolonged inhalation of large concentrations of dusts or particles that are considered relatively inert will also cause pulmonary neoplasms. The mechanism whereby these relatively nonreactive materials cause lung neoplasms is unknown. It has been speculated that the continued presence of heavy lung burden of inert material in the lung may induce neoplasms by chronic damage, repair, and inflammation.

Although considerable effort has been directed toward understanding the mechanism of neoplasm induction by asbestos, and much is known about fiber shape and size relative to neoplasm production, the basic mechanism is still open to speculation. Chrysotile is the most carcinogenic of the asbestos fibers in rats. Fibers with a diameter of less than 1.5  $\mu\text{m}$  and length greater than 8  $\mu\text{m}$  have the highest probability of neoplasm production. Many of the neoplasms induced by asbestos appear to be malignant, even when small, and many also appear to arise in a scar

or are associated with a scirrhous reaction. This pattern is not unique to asbestos but certainly is the most common pattern found in asbestos-induced carcinomas. Pleural mesotheliomas are induced by intrapleural injection of asbestos fibers and are rarely found in inhalation studies.

In the past, many studies used intratracheal instillation or direct injection of known carcinogens into the lung. These experiments often resulted in the development of squamous cell carcinomas even though they are very rare as a naturally occurring neoplasm. Instillation of chemicals or particles into the trachea or pleura or direct injection into the lung results in lesions or responses that may not be as relevant to understanding the mechanism of pulmonary carcinogenesis as inhalation of materials under more normal conditions. There remain, however, many areas where our understanding of the response of the lung to toxic chemicals is incomplete.

## REFERENCES

- Adamson, I.Y., Bowden, D.H., 1975. Derivation of type 1 epithelium from type 2 cells in the developing rat lung. *Lab. Investig.* 32, 736–745.
- Adriaensen, D., Brouns, I., Van Genechten, J., Timmermans, J.-P., 2003. Functional morphology of pulmonary neuroepithelial bodies: Extremely complex airway receptors. *The Anat. Rec. Part A: Discov. Mol. Cell. Evol. Biol.* 270A, 25–40.
- Alexander, I., Ritchie, B.C., Maloney, J.E., Hunter, C.R., 1975. Epithelial surfaces of the trachea and principal bronchi in the rat. *Thorax.* 30, 171–177.
- Almeida, O.Pd, Böhm, G.M., Carvalho, Md.P., Carvalho, A.Pd, 1975. The cardiac muscle in the pulmonary vein of the rat: a morphological and electrophysiological study. *J. Morphol.* 145, 409–433.
- Barthold, S.W., Griffey, S.M., Percy, D.H., 2016. *Rat, Pathology of Laboratory Rodents and Rabbits*. fourth edition John Wiley & Sons, Inc, Hoboken, New Jersey, USA, pp. 119–172.
- Besch-Williford, C., Pesavento, P., Hamilton, S., Bauer, B., Kapusinszky, B., Phan, T., et al., 2017. A naturally transmitted epitheliotropic polyomavirus pathogenic in immunodeficient rats: characterization, transmission, and preliminary epidemiologic studies. *Toxicol. Pathol.* 45, 593–603. Available from: <http://dx.doi.org/10.1177/0192623317723541>.
- Bienenstock, J., McDermott, M.R., 2005. Bronchus- and nasal-associated lymphoid tissues. *Immunol. Rev.* 206, 22–31.
- Bolender, R.P., Hyde, D.M., Dehoff, R.T., 1993. Lung morphometry: a new generation of tools and experiments for organ, tissue, cell, and molecular biology. *Am. J. Physiol.* 265, L521–L548.
- Bombard, E.M., 2017. Particle-induced pulmonary alveolar proteinosis and subsequent inflammation and fibrosis: a toxicologic and pathologic review. *Toxicol. Pathol.* 45, 389–401.
- Boorman, G.A., Brockmann, M., Carlton, W.W., Davis, J.M., Dungworth, D.L., Hahn, F.F., et al., 1996. Classification of cystic keratinizing squamous lesions of the rat lung: report of a workshop. *Toxicol. Pathol.* 24, 564–572.
- Boorman, G.A., Herbert, R., 1996. Alveolar/bronchiolar hyperplasia, adenoma and carcinoma, lung, rat. In: Jones, T.C., et al., (Eds.), *Monographs on Pathology of Laboratory Animals: Respiratory System*. Springer, Berlin, pp. 174–183.
- Boyd, M.R., 1984. Metabolic activation and lung toxicity: a basis for cell-selective pulmonary damage by foreign chemicals. *Environ. Health Perspect.* 55, 47–51.
- Brandsma, A.E., ten Have-Opbroek, A.A., Vulto, I.M., Molenaar, J.C., Tibboel, D., 1994. Alveolar epithelial composition and architecture of the late fetal pulmonary acinus: an immunocytochemical and morphometric study in a rat model of pulmonary hypoplasia and congenital diaphragmatic hernia. *Exp. Lung Res.* 20, 491–515.
- Brown, J.S., 2015. Chapter 27—Deposition of particles. In: Parent, R.A. (Ed.), *Comparative Biology of the Normal Lung*, second edition Academic Press, San Diego, pp. 513–536.
- Bucher, J., 1991. NTP technical report on the toxicity studies of cobalt sulfate heptahydrate in F344/N Rats and B6C3F1 mice (inhalation studies) (CAS No. 10026-24-1). *Toxic. Rep. Ser.* 5, 1-38.
- Burri, P.H., 1974. The postnatal growth of the rat lung III. Morphology. *Anat. Rec.* 180, 77–98.
- Burri, P.H., Moschopoulos, M., 1992. Structural analysis of fetal rat lung development. *Anat. Rec.* 234, 399–418.
- Cesta, M.F., 2006. Normal structure, function, and histology of mucosa-associated lymphoid tissue. *Toxicol. Pathol.* 34, 599–608.
- Chang, L.-Y., Mercer, R.R., Crapo, J.D., 1986. Differential distribution of brush cells in the rat lung. *Anat. Rec.* 216, 49–54.
- Crawford, J.M., Miller, D.A., 1984. Lymphocyte Subpopulations in Rat Lungs and Peyer's Patches. *Am. Rev. Respir. Dis.* 129, 827–832.
- Davis, J.M., 1979. The histopathology and ultrastructure of pleural mesotheliomas produced in the rat by injections of crocidolite asbestos. *Br. J. Exp. Pathol.* 60, 642–652.
- de Wet, C., Moss, J., 1998. Metabolic functions of the lung. *Anesthesiol. Clin. N. Am.* 16, 181–199.
- Dixon, D., Herbert, R.A., Kissling, G.E., Brix, A.E., Miller, R.A., Maronpot, R.R., 2008. Summary of chemically induced pulmonary lesions in the National Toxicology Program (NTP) toxicology and carcinogenesis studies. *Toxicol. Pathol.* 36, 428–439.
- Dixon, D., Maronpot, R.R., 1991. Histomorphologic features of spontaneous and chemically-induced pulmonary neoplasms in B6C3F1 mice and Fischer 344 rats. *Toxicol. Pathol.* 19, 540–556.
- Doi, T., Kotani, Y., Takahashi, K., Hashimoto, S., Yamada, N., Kokoshima, H., et al., 2010. Malignant mesothelioma in the thoracic cavity of a Crj:CD(SD) rat characterized by round hyaline stroma. *J. Toxicol. Pathol.* 23, 103–106.
- Dormans, J.A.M.A., 1983. The ultrastructure of various cell types in the lung of the rat: a survey. *Exp. Pathol.* 24, 15–33.
- Doster, A.R., Farrell, R.L., Wilson, B.J., 1983. An ultrastructural study of bronchiolar lesions in rats induced by 4-ipomeanol, a product from mold-damaged sweet potatoes. *Am. J. Pathol.* 111, 56–61.
- Edmondson, N.A., Lewis, D.J., 1980. Distribution and ultrastructural characteristics of Feyrter cells in the rat and hamster airway epithelium. *Thorax.* 35, 371–374.
- Elmore, S.A., Boyle, M.C., Boyle, M.H., Cora, M.C., Crabbs, T.A., Cummings, C.A., et al., 2014. Proceedings of the 2013 National Toxicology Program Satellite Symposium. *Toxicol. Pathol.* 42, 12–44.
- Evans, M.J., Johnson, L.V., Stephens, R.J., Freeman, G., 1976. Renewal of the terminal bronchiolar epithelium in the rat following exposure to NO<sub>2</sub> or O<sub>3</sub>. *Lab. Investig.* 35, 246–257.
- Everitt, J.I., Bermudez, E., Mangum, J.B., Wong, B., Moss, O.R., Janszen, D., et al., 1994. Pleural lesions in Syrian Golden Hamsters

- and Fischer-344 Rats following intrapleural instillation of man-made ceramic or glass fibers. *Toxicol. Pathol.* 22, 229–236.
- Everitt, J.L., Gelzleichter, T.R., Bermudez, E., Mangum, J.B., Wong, B.A., Janszen, D.B., et al., 1997. Comparison of pleural responses of rats and hamsters to subchronic inhalation of refractory ceramic fibers. *Environ. Health Perspect.* 105, 1209–1213.
- Ferreira, P., Silva, A., Aguas, A., Pereira, A., Grande, N., 2001. Detailed arrangement of the bronchial arteries in the Wistar rat: a study using vascular injection and scanning electron microscopy. *Eur. J. Anat.* 5, 67–76.
- Genechten, J.V., Brouns, I., Burnstock, G., Timmermans, J.-P., Adriaensens, D., 2004. Quantification of neuroepithelial bodies and their innervation in fawn-hooded and Wistar rat lungs. *Am. J. Respir. Cell Mol. Biol.* 30, 20–30.
- Gosney, J.R., Sissons, M.C., 1985. Widespread distribution of bronchopulmonary endocrine cells immunoreactive for calcitonin in the lung of the normal adult rat. *Thorax.* 40, 194–198.
- Gram, T.E., 1989. *Pulmonary toxicity of 4-ipomeanol*. *Pharmacol. Ther.* 43, 291–297.
- Greaves, P., Chouinard, L., Ernst, H., Mecklenburg, L., Pruijboom-brees, I.M., Rinke, M., et al., 2013. Proliferative and non-proliferative lesions of the rat and mouse soft tissue, skeletal muscle and mesothelium. *J. Toxicol. Pathol.* 26, 1S–26S.
- Guilbert, T.W., Gebb, S.A., Shannon, J.M., 2000. Lung hypoplasia in the nitrofen model of congenital diaphragmatic hernia occurs early in development. *Am. J. Physiol. Lung Cell. Mol. Physiol.* 279, L1159–L1171.
- Guilliams, M., De Kleer, I., Henri, S., Post, S., Vanhoutte, L., De Prijck, S., et al., 2013. Alveolar macrophages develop from fetal monocytes that differentiate into long-lived cells in the first week of life via GM-CSF. *J. Exp. Med.* 210, 1977–1992.
- Haschek, W.M., Morse, C.C., Boyd, M.R., Hakkinen, P.J., Witschi, H.P., 1983. Pathology of acute inhalation exposure to 3-methylfuran in the rat and hamster. *Exp. Mol. Pathol.* 39, 342–354.
- Haworth, R., Woodfine, J., McCawley, S., Pilling, A.M., Lewis, D.J., Williams, T.C., 2007. Pulmonary neuroendocrine cell hyperplasia: identification, diagnostic criteria and incidence in untreated ageing rats of different strains. *Toxicol. Pathol.* 35, 735–740.
- Hebel, R., Stromberg, M., 1976. *Anatomy of the Laboratory Rat*. The Williams and Wilkins Company, Baltimore.
- Henderson, K.S., Dole, V., Parker, N.J., Momtsios, P., Banu, L., Brouillette, R., et al., 2012. *Pneumocystis carinii* causes a distinctive interstitial pneumonia in immunocompetent laboratory rats that had been attributed to “rat respiratory virus”. *Vet. Pathol.* 49, 440–452.
- Herbert, R.A., Stegelmeier, B.S., Gillett, N.A., Rebar, A.H., Carlton, W.W., Singh, G., et al., 1994. Plutonium-induced proliferative lesions and pulmonary epithelial neoplasms in the rat: immunohistochemical and ultrastructural evidence for their origin from type II pneumocytes. *Vet. Pathol.* 31, 366–374.
- Hislop, A., Reid, L., 1978. Normal structure and dimensions of the pulmonary arteries in the rat. *J. Anat.* 125, 71–83.
- Hofmann, W., Bálásházy, I., Heistracher, T., Koblinger, L., 1996. The significance of particle deposition patterns in bronchial airway bifurcations for extrapolation modeling. *Aerosol Sci. Technol.* 25, 305–327.
- Hook, G.E., 1991. Alveolar proteinosis and phospholipidoses of the lungs. *Toxicol. Pathol.* 19, 482–513.
- Hosoyamada, Y., Ichimura, K., Koizumi, K., Sakai, T., 2010. Structural organization of pulmonary veins in the rat lung, with special emphasis on the musculature consisting of cardiac and smooth muscles. *Anat. Sci. Int.* 85, 152–159.
- Howroyd, P., Allison, N., Foley, J.F., Hardisty, J., 2009. Apparent alveolar bronchiolar tumors arising in the mediastinum of F344 rats. *Toxicol. Pathol.* 37, 351–358.
- Ike, F., Sakamoto, M., Ohkuma, M., Kajita, A., Matsushita, S., Kokubo, T., 2016. *Filobacterium rodentium* gen. nov., sp. nov., a member of Filobacteriaceae fam. nov. within the phylum Bacteroidetes; includes a microaerobic filamentous bacterium isolated from specimens from diseased rodent respiratory tracts. *Int. J. Syst. Evol. Microbiol.* 66, 150–157.
- Jeffery, P.K., Reid, L., 1975. New observations of rat airway epithelium: a quantitative and electron microscopic study. *J. Anat.* 120, 295–320.
- Joseph, D., Puttaswamy, R.K., Krovvidi, H., 2013. Non-respiratory functions of the lung. *Contin. Educ. Anaesth. Crit. Care Pain.* 13, 98–102.
- Kane, A.B., 2006. Animal models of malignant mesothelioma. *Inhal. Toxicol.* 18, 1001–1004.
- Kast, A., 1996. Pulmonary hair embolism, rat. In: Jones, T.C., et al., (Eds.), *Respiratory System*. Springer Berlin Heidelberg, Berlin, Heidelberg, pp. 293–302.
- Kay, J.M., 2015. Appendix 3—Blood vessels of the lung. In: Parent, R. A. (Ed.), *Comparative Biology of the Normal Lung*, second edition Academic Press, San Diego, pp. 759–768.
- Kim, H.-S., Do, S.-I., Kim, Y.W., 2014. Histopathology of *Pneumocystis carinii* pneumonia in immunocompetent laboratory rats. *Exp. Ther. Med.* 8, 442–446.
- Kittel, B., 1996. Goblet cell metaplasia, lung, rat. In: Jones, T.C., et al., (Eds.), *Respiratory System*. Springer Berlin Heidelberg, Berlin, Heidelberg, pp. 303–307.
- Lane, B.P., Zeidler, M., Weinhold, C., Drummond, E., 1983. Organization and structure of branches in the rat pulmonary arterial bed. *Anat. Rec.* 205, 397–403.
- Laskin, D.L., Malaviya, R., Laskin, J.D., 2015. Chapter 32—Pulmonary macrophages. In: Parent, R.A. (Ed.), *Comparative Biology of the Normal Lung*, second edition Academic Press, San Diego, pp. 629–649.
- Laskin, D.L., Sunil, V.R., Gardner, C.R., Laskin, J.D., 2011. Macrophages and tissue injury: agents of defense or destruction? *Annu. Rev. Pharmacol. Toxicol.* 51, 267–288.
- Leak, L.V., 1980. Lymphatic removal of fluids and particles in the mammalian lung. *Environ. Health Perspect.* 35, 55–75.
- Leak, L.V., Jamuar, M.P., 1983. Ultrastructure of pulmonary lymphatic vessels. *Am. Rev. Respir. Dis.* 128, S59–S65.
- Lehnert, B.E., Valdez, Y.E., Holland, L.M., 1985. Pulmonary macrophages: alveolar and interstitial populations. *Exp. Lung Res.* 9, 177–190.
- Livingston, R.S., Besch-Williford, C.L., Myles, M.H., Franklin, C.L., Crim, M.J., Riley, L.K., 2011. *Pneumocystis carinii* infection causes lung lesions historically attributed to rat respiratory virus. *Comp. Med.* 61, 45–59.
- Lum, H., Schwartz, L.W., Dungworth, D.L., Tyler, W.S., 1978. A comparative study of cell renewal after exposure to ozone or oxygen. *Am. Rev. Respir. Dis.* 118, 335–345.

- Marin, M.L., Lane, B.P., Gordon, R.E., Drummond, E., 1979. Ultrastructure of rat tracheal epithelium. *Lung*. 156, 223–236.
- McAteer, J.A., 1984. Tracheal morphogenesis and fetal development of the mucociliary epithelium of the rat. *Scan. Electron Microsc.* 1995–2008.
- McLaughlin Jr., R.F., 1983. Bronchial artery distribution in various mammals and in humans. *Am. Rev. Respir. Dis.* 128, S57–S58.
- Mercer, R.R., Russell, M.L., Roggli, V.L., Crapo, J.D., 1994. Cell number and distribution in human and rat airways. *Am. J. Respir. Cell Mol. Biol.* 10, 613–624.
- Meyrick, B., Hislop, A., Reid, L., 1978. Pulmonary arteries of the normal rat: the thick walled oblique muscle segment. *J. Anat.* 125, 209–221.
- Meyrick, B., Reid, L., 1968. The alveolar brush cell in rat lung—a third pneumonocyte. *J. Ultrastruct. Res.* 23, 71–80.
- Miller, B.E., Hook, G.E., 1990. Hypertrophy and hyperplasia of alveolar type II cells in response to silica and other pulmonary toxicants. *Environ. Health Perspect.* 85, 15–23.
- Misharin, A.V., Morales-Nebreda, L., Reyfman, P.A., Cuda, C.M., Walter, J.M., McQuattie-Pimentel, A.C., et al., 2017. Monocyte-derived alveolar macrophages drive lung fibrosis and persist in the lung over the life span. *J. Exp. Med.* 214, 2387–2404.
- Mohr, U., Ernst, H., Roller, M., Pott, F., 2006. Pulmonary tumor types induced in Wistar rats of the so-called “19-dust study”. *Exp. Toxicol. Pathol.* 58, 13–20.
- Morgan, D.L., Jokinen, M.P., Johnson, C.L., Price, H.C., Gwinn, W.M., Bousquet, R.W., et al., 2016. Chemical reactivity and respiratory toxicity of the  $\alpha$ -diketone flavoring agents. *Toxicol. Pathol.* 44, 763–783.
- Morse, D.E., Gattone, V.H., McCann, P., 1979. Surface features of the developing rat lung. *Scan. Electron Microsc.*(3), 899–904, 842.
- Nakakuki, S., 1983. The bronchial tree and blood vessels of the rat lung. *Anat. Anz.* 154, 305–312.
- NTP, 1994. NTP toxicology and carcinogenesis studies of ozone (CAS No. 10028-15-6) and Ozone/NNK (CAS No. 10028-15-6/ 64091-91-4) in F344/N rats and B6C3F1 mice (inhalation studies). *Natl. Toxicol. Program Tech. Rep. Ser.* 440, 1–314.
- NTP, 1996a. NTP toxicology and carcinogenesis studies of nickel subsulfide (CAS No. 12035-72-2) in F344 rats and B6C3F1 mice (inhalation studies). *Natl. Toxicol. Program Tech. Rep. Ser.* 453, 1–365.
- NTP, 1996b. NTP toxicology and carcinogenesis studies of nickel sulfate hexahydrate (CAS No. 10101-97-0) in F344 rats and B6C3F1 mice (inhalation studies). *Natl. Toxicol. Program Tech. Rep. Ser.* 454, 1–380.
- NTP, 2000. NTP toxicology and carcinogenesis studies of gallium arsenide (CAS No. 1303-00-0) in F344/N rats and B6C3F1 mice (inhalation studies). *Natl. Toxicol. Program Tech. Rep. Ser.* 492, 1–306.
- NTP, 2001. Toxicology and carcinogenesis studies of indium phosphide (CAS No. 22398-90-7) in F344/N rats and B6C3F1 mice (inhalation studies). *Natl. Toxicol. Program Tech. Rep. Ser.* 7–340.
- Ohshima, M., Ward, J.M., Singh, G., Katyal, S.L., 1985. Immunocytochemical and morphological evidence for the origin of *N*-nitrosomethylurea-induced and naturally occurring primary lung tumors in F344/NCr rats. *Cancer Res.* 45, 2785–2792.
- Ohtsuka, R., Doi, K., Itagaki, S., 1997. Histological characteristics of respiratory system in Brown Norway rat. *Exp. Anim.* 46, 127–133.
- Oliveira, M.J.R., Pereira, A.S., Guimarães, L., Grande, N.R., Moreira de Sá, C., Águas, A.P., 2003. Zonation of ciliated cells on the epithelium of the rat trachea. *Lung*. 181, 275–282.
- Otsuki, Y., Ito, Y., Magari, S., 1989. Lymphocyte subpopulations in high endothelial venules and lymphatic capillaries of bronchus-associated lymphoid tissue (BALT) in the rat. *Am. J. Anat.* 184, 139–146.
- Otto, G.M., Franklin, C.L., Clifford, C.B., 2015. Chapter 4—Biology and diseases of rats, *Laboratory Animal Medicine*. Third edition Academic Press, Boston, pp. 151–207.
- Pabst, R., Gehrke, I., 1990. Is the bronchus-associated lymphoid tissue (BALT) an integral structure of the lung in normal mammals, including humans? *Am. J. Respir. Cell Mol Biol.* 3, 131–135.
- Pan, J., Park, T.J., Cutz, E., Yeger, H., 2014. Immunohistochemical characterization of the chemosensory pulmonary neuroepithelial bodies in the naked mole-rat reveals a unique adaptive phenotype. *PLoS One.* 9, e112623.
- Peake, J.L., Pinkerton, K.E., 2015. Chapter 3—Gross and subgross anatomy of lungs, pleura, connective tissue septa, distal airways, and structural units. In: Parent, R.A. (Ed.), *Comparative Biology of the Normal Lung*, second edition Academic Press, San Diego, pp. 21–31.
- Pinkerton, K.E., Barry, B.E., O’Neil, J.J., Raub, J.A., Pratt, P.C., Crapo, J.D., 1982. Morphologic changes in the lung during the lifespan of Fischer 344 rats. *Am. J. Anat.* 164, 155–174.
- Pinkerton, K.E., Van Winkle, L.S., Plopper, C.G., Smiley-Jewell, S., Covarrubias, E.C., McBride, J.T., et al., 2015. Chapter 4—Architecture of the tracheobronchial tree. In: Parent, R.A. (Ed.), *Comparative Biology of the Normal Lung*, second edition Academic Press, San Diego, pp. 33–51.
- Plopper, C.G., 1983. Comparative morphologic features of bronchiolar epithelial cells. *Am. Rev. Respir. Dis.* 128, S37–S41.
- Plopper, C.G., Hyde, D.M., 2015. Chapter 7—Epithelial cells of the bronchiole. In: Parent, R.A. (Ed.), *Comparative Biology of the Normal Lung*, second edition Academic Press, San Diego, pp. 83–92.
- Plopper, C.G., Mariassy, A.T., Wilson, D.W., Alley, J.L., Nishio, S.J., Nettesheim, P., 1983. Comparison of nonciliated tracheal epithelial cells in six mammalian species: ultrastructure and population densities. *Exp. Lung Res.* 5, 281–294.
- Porter, D.W., Ramsey, D., Hubbs, A.F., Battelli, L., Ma, J., Barger, M., et al., 2001. Time course of pulmonary response of rats to inhalation of crystalline silica: histological results and biochemical indices of damage, lipidosis, and fibrosis. *J. Environ. Pathol. Toxicol. Oncol.* 20, 1–14.
- Rehm, S., 1996. Comparative aspects of pulmonary carcinogenesis. In: Jones, T.C., et al., (Eds.), *Monographs on Pathology of Laboratory Animals: Respiratory System*. Springer, Heidelberg, pp. 158–173.
- Reid, L., Meyrick, B., Antony, V.B., Chang, L.-Y., Crapo, J.D., Reynolds, H.Y., 2005. The mysterious pulmonary brush cell. *Am. J. Respir. Crit. Care Med.* 172, 136–139.
- Renne, R., Brix, A., Harkema, J., Herbert, R., Kittel, B., Lewis, D., et al., 2009. Proliferative and nonproliferative lesions of the rat and mouse respiratory tract. *Toxicol. Pathol.* 37, 5S–73S.
- Renne, R., Fouillet, X., Maurer, J., Assaad, A., Morgan, K., Ha, F., et al., 2001. Recommendation of optimal method for formalin fixation of rodent lungs in routine toxicology studies. *Toxicol. Pathol.* 29, 587–589.
- Reynolds, S.D., Malkinson, A.M., 2010. *Clara cell: progenitor* for the bronchiolar epithelium. *Int. J. Biochem. Cell Biol.* 42, 1–4.

- Reynolds, S.D., Pinkerton, K.E., Mariassy, A.T., 2015. Chapter 6—Epithelial cells of trachea and bronchi. In: Parent, R.A. (Ed.), *Comparative Biology of the Normal Lung*, second edition Academic Press, San Diego, pp. 61–81.
- Reznik-Schuller, H.M., Reznik, G., 1982. Morphology of spontaneous and induced tumors in the bronchiolo-alveolar region of F344 rats. *Anticancer Res.* 2, 53–57.
- Rittinghausen, S., Kaspereit, J., 1998. Spontaneous cystic keratinizing epithelioma in the lung of a Sprague-Dawley rat. *Toxicol. Pathol.* 26, 298–300.
- Rittinghausen, S., Mohr, U., Dungworth, D.L., 1997. Pulmonary cystic keratinizing squamous cell lesions of rats after inhalation/instillation of different particles. *Exp. Toxicol. Pathol.* 49, 433–446.
- Schlesinger, R.B., McFadden, L.A., 1981. Comparative morphometry of the upper bronchial tree in six mammalian species. *Anat. Rec.* 199, 99–108.
- Schoeb, T.R., McConnell, E.E., Juliana, M.M., Davis, J.K., Davidson, M.K., Lindsey, J.R., 2009a. *Mycoplasma pulmonis* and lymphoma. *Environ. Mol. Mutagen.* 50, 1–3.
- Schoeb, T.R., McConnell, E.E., Juliana, M.M., Davis, J.K., Davidson, M.K., Lindsey, J.R., 2009b. *Mycoplasma pulmonis* and lymphoma in bioassays in rats. *Vet. Pathol.* 46, 952–959.
- Schwartz, L.W., 1986. Pulmonary responses to inhaled irritants and the morphological evaluation of those responses. In: Salem, H. (Ed.), *Inhalation Toxicology: Research Methods, Applications, and Evaluation*. Marcel Dekker, New York, pp. 293–347.
- Seymour, J.F., Presneill, J.J., 2002. Pulmonary alveolar proteinosis. *Am. J. Respir. Crit. Care Med.* 166, 215–235.
- Shellito, J., Esparza, C., Armstrong, C., 1987. Maintenance of the normal rat alveolar macrophage cell population. The roles of monocyte influx and alveolar macrophage proliferation in situ. *Am. Rev. Respir. Dis.* 135, 78–82.
- Singh, G., Katyal, S.L., 2000. Clara cell proteins. *Annals of the New York Academy of Sciences.* 923, 43–58.
- Sminia, T., van der Brugge-Gamelkoorn, G., van der Ende, M., 1990. Bronchus-associated lymphoid tissue, rat, normal structure. In: Jones, T.C., et al., (Eds.), *Monographs on Pathology of Laboratory Animals: Hematopoietic System*. Springer-Verlag, New York, pp. 300–307.
- Sorokin, S.P., Hoyt, R.F., Grant, M.M., 1984. Development of macrophages in the lungs of fetal rabbits, rats, and hamsters. *Anat. Rec.* 208, 103–121.
- Spicer, S.S., Setser, M.E., Mochizuki, I., Simson, J.A.V., 1982. The histology and fine structure of glands in the rat respiratory tract. *Anat. Rec.* 202, 33–43.
- Spritzer, A.A., Watson, J.A., Auld, J.A., Guetthoff, M.A., 1968. Pulmonary macrophage clearance. The hourly rates of transfer of pulmonary macrophages to the oropharynx of the rat. *Arch. Environ. Health.* 17, 726–730.
- Stanton, M.F., Wrench, C., 1972. Mechanisms of mesothelioma induction with asbestos and fibrous glass. *JNCI: J. Natl. Cancer Inst.* 48, 797–821.
- Stringer, J.R., 1993. The identity of *Pneumocystis carinii*: not a single protozoan, but a diverse group of exotic fungi. *Infect. Agents Dis.* 2, 109–117.
- Touya, J.J., Rahimian, J., Corbus, H.F., Grubbs, D.E., Savala, K.M., Glass, E.C., et al., 1986. The lung as a metabolic organ. *Sem. Nucl. Med.* 16, 296–305.
- Vidic, B., Burri, P.H., 1983. Morphometric analysis of the remodeling of the rat pulmonary epithelium during early postnatal development. *Anat. Rec.* 207, 317–324.
- Wagner, J.C., 1962. Experimental production of mesothelial tumours of the pleura by implantation of dusts in laboratory animals. *Nature.* 196, 180–181.
- Wagner, J.C., Berry, G., 1969. Mesotheliomas in rats following inoculation with asbestos. *Br. J. Cancer.* 23, 567–581.
- Walker, N.J., Yoshizawa, K., Miller, R.A., Brix, A.E., Sells, D.M., Jokinen, M.P., et al., 2007. Pulmonary lesions in female Harlan Sprague-Dawley rats following two-year oral treatment with dioxin-like compounds. *Toxicol. Pathol.* 35, 880–889.
- Warburton, D., El-Hashash, A., Carraro, G., Tiozzo, C., Sala, F., Rogers, O., et al., 2010. Chapter three—Lung organogenesis. In: Peter, K. (Ed.), *Current Topics in Developmental Biology*, vol. 90. Academic Press, New York, pp. 73–158.
- Weibel, E.R., Hsia, C.C.W., Ochs, M., 2007. How much is there really? Why stereology is essential in lung morphometry. *J. Appl. Physiol.* 102, 459–467.
- Widdicombe, J.H., Chen, L.L.K., Sporer, H., Choi, H.K., Pecson, I.S., Bastacky, S.J., 2001. Distribution of tracheal and laryngeal mucous glands in some rodents and the rabbit. *J. Anat.* 198, 207–221.
- Yamada, T., Suzuki, E., Gejyo, F., Ushiki, T., 2002. Developmental changes in the structure of the rat fetal lung, with special reference to the airway smooth muscle and vasculature. *Arch. Histol. Cytol.* 65, 55–69.
- Yeh, H.C., Phalen, R.F., Raabe, O.G., 1976. Factors influencing the deposition of inhaled particles. *Environ. Health Perspect.* 15, 147–156.
- Yeh, H.C., Schum, G.M., Duggan, M.T., 1979. Anatomic models of the tracheobronchial and pulmonary regions of the rat. *Anat. Rec.* 195, 483–492.
- Zhang, J.Y., Wang, Y., Prakash, C., 2006. Xenobiotic-metabolizing enzymes in human lung. *Curr. Drug Metab.* 7, 939–948.